TABLE 1. (CONTINUED)

Description	Genes	Accession Numbers
Myc associated factor X dimerization protein 1	*MXD1*	NM_002357
cDNA MR0-RT0026-160401-104-h09 RT0026	*BI009763*	BI009763
Glutamate receptor interacting protein and coiled-coil domain containing 2	*GCC2*	NM_181453
Transmembrane emp24-like trafficking protein 10 (yeast) pseudogene	*TMED10P*	AJ004914
Special AT-rich sequence-binding protein homeobox 1	*SATB1*	NM_002971
Zinc finger CCCH-type containing 7A	*ZC3H7A*	NM_014153
Toll interacting protein	*TOLLIP*	NM_019009
cDNA FLJ13707 fis, clone PLACE2000347	*STAMBP*	AK023769
Ninein (GSK3B interacting protein)	*NIN*	NM_016350
Melanoma inhibitory activity family, member 3	*MIA3*	AK096526
Ras-related protein 1 GTPase-activating protein	*RAP1GAP*	NM_002885
Elongation factor Tu GTP binding domain containing 1	*EFTUD1*	NM_024580
Suppressor of Ty, domain containing 1 (*Saccharomyces cerevisiae*)	*SPTY2D1*	NM_194285
Hepatoma-derived growth factor, related protein 3	*HDGFRP3*	NM_016073
RNA binding motif protein 22	*RBM22*	NM_018047
Calcium/calmodulin-dependent serine protein kinase interacting protein 2	*CASKIN2*	NM_020753
Ras association (RalGDS/AF-6) and pleckstrin homology domains 1	*RAPH1*	NM_213589
Hypothetical protein LOC286272	*LOC286272*	AK000939
Transmembrane protease, serine 3	*TMPRSS3*	NM_032401
Coiled-coil domain containing 66	*CCDC66*	NM_001012506
Solute carrier family 45, member 4	*SLC45A4*	AB032952
cDNA clone: 3948082	*NOS1*	BC010126
Iroquois homeobox 5	*IRX5*	NM_005853
Organic solute transporter–β	*OSTbeta*	NM_178859
Hypothetical protein FLJ10404	*FLJ10404*	NM_019057
Regulating synaptic membrane exocytosis 3	*RIMS3*	NM_014747
Chorionic gonadotropin, β-polypeptide 1	*CGB1*	NM_033377
Secreted frizzled-related protein 1	*SFRP1*	NM_003012
Cysteine-rich secretory protein Limulus factor C, Coch-5b2 and Lgl1 domain–containing 2	*CRISPLD2*	BC007689
Protein phosphatase 1F (PP2C domain containing)	*PPM1F*	NM_014634
Steroidogenic acute regulatory protein-related lipid transfer (START) domain–containing 13	*STARD13*	NM_178006
Phospholipase C, β2	*PLCB2*	NM_004573
Glucosyltransferases, Rab-like GTPase activators and Myotubularins domain–containing 1C	*GRAMD1C*	NM_017577
cDNA clone: 998I221826	*BX119852*	BX119852
Replication protein A4, 34 kD	*RPA4*	NM_013347
Calcium-binding protein 7	*CABP7*	NM_182527
Golgin-like hypothetical protein LOC440321	*FLJ32679*	NM_001012452
Leucine-rich repeat–containing 2	*LRRC2*	NM_024512
Solute carrier family 10 (sodium/bile acid cotransporter family), member 1	*SLC10A1*	NM_003049
Tryptophan-aspartic acid repeat domain 33	*WDR33*	NM_018383
cDNA clone: 277235	*N47124*	N47124
Phosphoinositide-3–kinase, regulatory subunit 5	*PIK3R5*	NM_014308
Insulin-like growth factor binding protein 3	*IGFBP3*	NM_001013398
Dystrophin	*dystrophin*	S71486
Growth factor receptor bound protein 2-associated binding protein 2	*GAB2*	NM_012296
Carbonic anhydrase II	*CA2*	NM_000067
A kinase anchor protein 12	*AKAP12*	NM_144497
cDNA clone: 450936	*AA704712*	AA704712
Insulin-like growth factor 2 mRNA binding protein 2	*IGF2BP2*	NM_006548
Cystatin A (stefin A)	*CSTA*	NM_005213
Septin 1	*SEPT1*	NM_052838
Tight junction protein 1 (zona occludens 1)	*TJP1*	NM_003257
Coiled-coil domain containing 88A	*CCDC88A*	NM_018084
cDNA DKFZp686J1595	*BX538057*	BX538057
Chromosome 5 open reading frame 39	*C5orf39*	NM_001014279
Calcium-binding protein 39-like	*CAB39L*	NM_030925
Transmembrane protein 56	*TMEM56*	NM_152487
Tryptophan-tryptophan domain containing oxidoreductase	*WWOX*	NM_130844
FLJ35767 protein	*FLJ35767*	NM_207459
Riboflavin kinase	*RFK*	NM_018339
Stress-associated endoplasmic reticulum protein family member 2	*SERP2*	NM_001010897
Dehydrogenase/reductase member 9	*DHRS9*	NM_005771
Teashirt zinc finger homeobox 1	*TSHZ1*	NM_005786
Nance-Horan syndrome-like 1	*NHSL1*	AB037778
Solute carrier family 39 (zinc transporter), member 6	*SLC39A6*	NM_012319
Zinc finger, Cysteine-cysteine-histidine-cysteine domain–containing 2	*ZCCHC2*	BC006340
Zinc-binding alcohol dehydrogenase domain–containing 2	*ZADH2*	NM_175907
Pentraxin-related gene, rapidly induced by IL-1β	*PTX3*	NM_002852
Family with sequence similarity 124B	*FAM124B*	NM_024785
Forkhead box F2	*FOXF2*	NM_001452

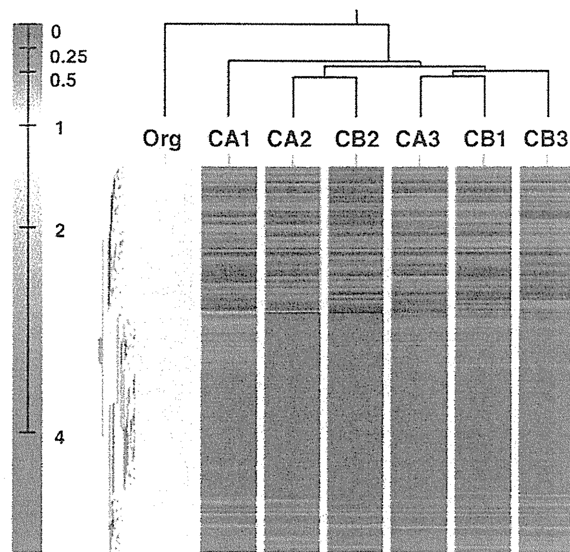

Figure 3. Clustering analysis of 139 genes reveals differences between MT-2Org and MT-2Rsts cells. Expression is scaled so that *green* represents low expression, and *red* represents high expression.

data were processed by the MetaCore system, which allows the visualization of microarray data on canonical pathways and the construction of gene networks using pathway and network analysis. The top 30 results of the pathway analysis are listed in Table 2. We focused on the suppression of the IFN-γ signaling pathway, because the production of IFN-γ was shown to decrease in CB1 cells compared with MT-2Org cells (17), and IFN-γ is considered one of the most important cytokines for organizing tumor rejection by immunocompetent cells. The expression of two genes, IFN regulatory factor 9 (*IRF9*) and IFN-stimulated gene factor–3 (*ISGF3*), was significantly reduced in all MT-2Rsts cells exposed continuously to CA or CB (Figure 4). In addition, the build networks from the 139 genes indicated that the decreased expression of CXCR3 in all MT-2Rsts cells was regulated by *IRF9* through CXCL10/IP-10 (Figure 5). Therefore, the cell-surface expression of CXCR3 was thought to be important among the cellular and molecular alterations in MT-2Rsts cells continuously exposed to asbestos.

Decline of Th1-Type CXCR3 Expression, IFN-γ Production, and CXCL10/IP10 Production in MT-2Rsts Cells Chronically Exposed to Chrysotile Asbestos

Because the expression of CXCR3 and production of IFN-γ are known to be induced by T-cell activation and lead to the enhancement of antitumor immune function (22), we investigated the expression of the Th1-type chemokine receptor CXCR3 and cytokine IFN-γ. As shown in Figure 6A, the cell-surface expression of CXCR3 was examined in gated live cells on MT-2Org and MT-2Rsts cells. All MT-2Rsts cells showed a reduction of cell-surface CXCR3-positive cells, although no significant difference was evident between MT-2Org and CB2 cells, as indicated by real-time RT-PCR (Figure 6B). Furthermore, all MT-2Rsts cells showed less production of IFN-γ compared with MT-2Org cells (Figure 7A). These findings support the notion that the down-regulation of Th1-type molecules CXCR3 and IFN-γ is important in recognizing the immunologic effect of asbestos.

As shown in Figure 7B, the production of the Th1-type CXCR3 ligand CXCL10/IP10 was also significantly reduced in all MT-2Rsts cells compared with MT-2Org cells. In addition, another Th1-type chemokine, *CCL4*/ *MIP-1*β mRNA, was also expressed at low concentrations in all MT-2Rsts cells compared

TABLE 2. PATHWAY RESULTS

Map	*P* values[a]
1. Phosphatidylinositol-3,4,5-trisphosphate signaling in B lymphocytes	5.22E-03
2. IFN-α/β signaling pathway	9.05E-03
3. Regulation of lipid metabolism G-α(q) regulation of lipid metabolism	1.55E-02
4. Inhibitory action of lipoxins on superoxide production in neutrophils	1.95E-02
5. Angiotensin signaling via signal transducers and activators of transcription	1.95E-02
6. Transcription factor Tubby signaling pathways	2.62E-02
7. Transcription regulation of granulocyte development	3.46E-02
8. Apoptosis and survival–β-2 adrenergic receptor antiapoptotic action	4.71E-02
9. Membrane trafficking and signal transduction of G-α (i) heterotrimeric G-protein	5.30E-02
10. Gap junctions	9.35E-02
11. G-protein–β/γ signaling cascades	1.01E-01
12. Macrophage migration inhibitory factor, the neuroendocrine-macrophage connector	1.32E-01
13. α-2 adrenergic receptor regulation of ion channels	1.40E-01
14. Antiviral actions of interferons	1.65E-01
15. Calcium signaling	1.74E-01
16. Extracellular signal–regulated kinase interactions: inhibition of extracellular signal–regulated kinases	1.82E-01
17. G-protein–mediated regulation mitogen-activated protein kinase-extracellular signal–regulated kinase signaling	1.91E-01
18. Endothelin receptor type B signaling	1.91E-01
19. A1 receptor signaling	2.00E-01
20. A3 receptor signaling	2.00E-01
21. G-protein–mediated regulation p38 and c-Jun N-terminal kinase signaling	2.00E-01
22. Inducible costimulator-Inducible costimulator ligand pathway in T-helper cells	2.09E-01
23. Histamine H1 receptor signaling in the interruption of cell-barrier integrity	2.17E-01
24. Inhibitory action of lipoxins on neutrophil migration	2.17E-01
25. Histamine signaling in dendritic cells	2.35E-01
26. Activation of protein kinase C via G-protein–coupled receptor	2.35E-01
27. Inositol 1,4,5-triphosphate signaling	2.44E-01
28. Role of vitamin D receptor in regulation of genes involved in osteoporosis	2.80E-01
29. IFN-γ signaling pathway	2.89E-01
30. G protein-coupled receptors in platelet aggregation	3.42E-01

[a]*P* values is calculated by comparing the number of interest genes that participate in a given pathway, relative to the total number of occurrences of these genes in all pathway annotations stored in the Metacore database.

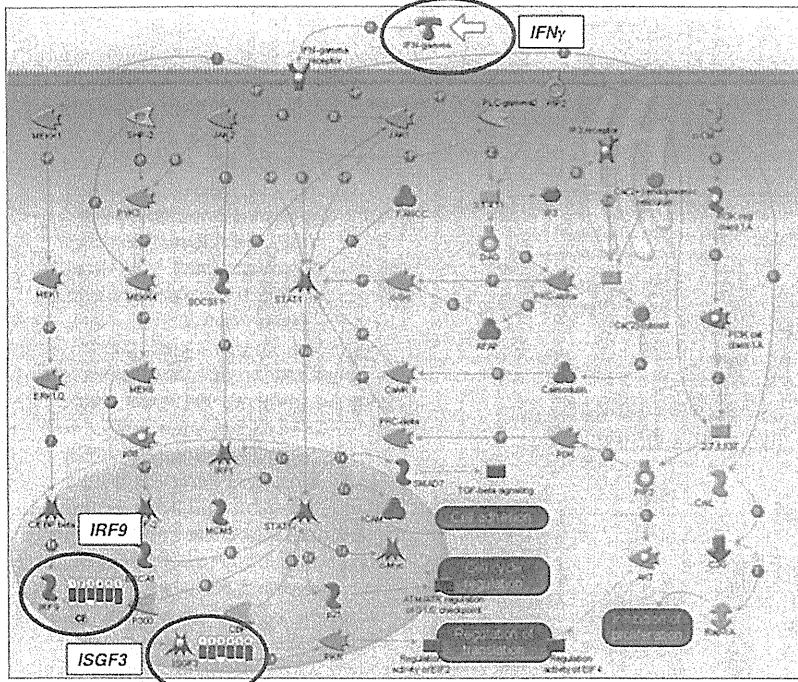

Figure 4. IFN-γ signaling canonical pathway analysis shows that the expression of *IRF9* and *ISGF3* is down-regulated in MT-2Rsts cells. *Blue thermometers* indicate down-regulation. Numbers indicate cell line names (2, CA1; 3, CA2; 4, CA3; 5, CB1; 6, CB2; 7, CB3).

with MT-2Org cells (Table 1 and Figure 7C). However, CCR5, the Th1-type receptor for CCL4/MIP-1β, was not reduced significantly through the expression of mRNA in MT-2Rsts cells (Figure 7C). These results indicate that a continuous exposure of MT-2Org cells to asbestos altered the expression of Th1-related chemokines (CXCL10/IP10 and CCL4/MIP-1β) and chemokine receptors (CXCR3).

DISCUSSION

Pneumoconiosis is an occupational and restrictive set of lung diseases caused by the inhalation of dust, often in mines (23–26), and typically including silicosis and asbestosis. Silicosis is caused by the inhalation of crystalline silica dust, and is marked by inflammation and scarring in the form of nodular lesions in the upper lobes of lungs. On the other hand, asbestosis is a chronic inflammatory and fibrotic medical condition affecting the parenchymal tissue of the lungs, and is caused by the inhalation and retention of asbestos fibers. It usually occurs after high-intensity or long-term exposure to asbestos, particularly in individuals working on the production or end-use of products containing asbestos (23–26). Patients with silicosis suffer not only from respiratory dysfunction, but sometimes from complications involving autoimmune diseases such as rheumatoid arthritis

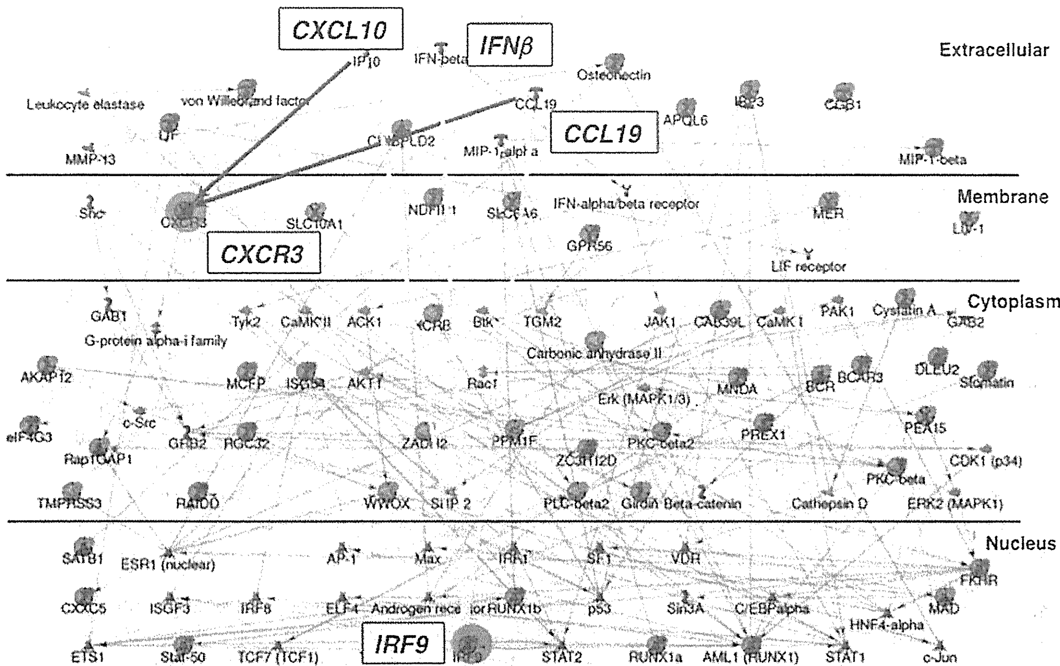

Figure 5. Network analysis indicates that down-regulation of *CXCR3* is regulated by *IRF9*. *Blue circles* indicate reduced genes. *Green arrows* and *gray arrows* indicate positive and unspecified effects, respectively.

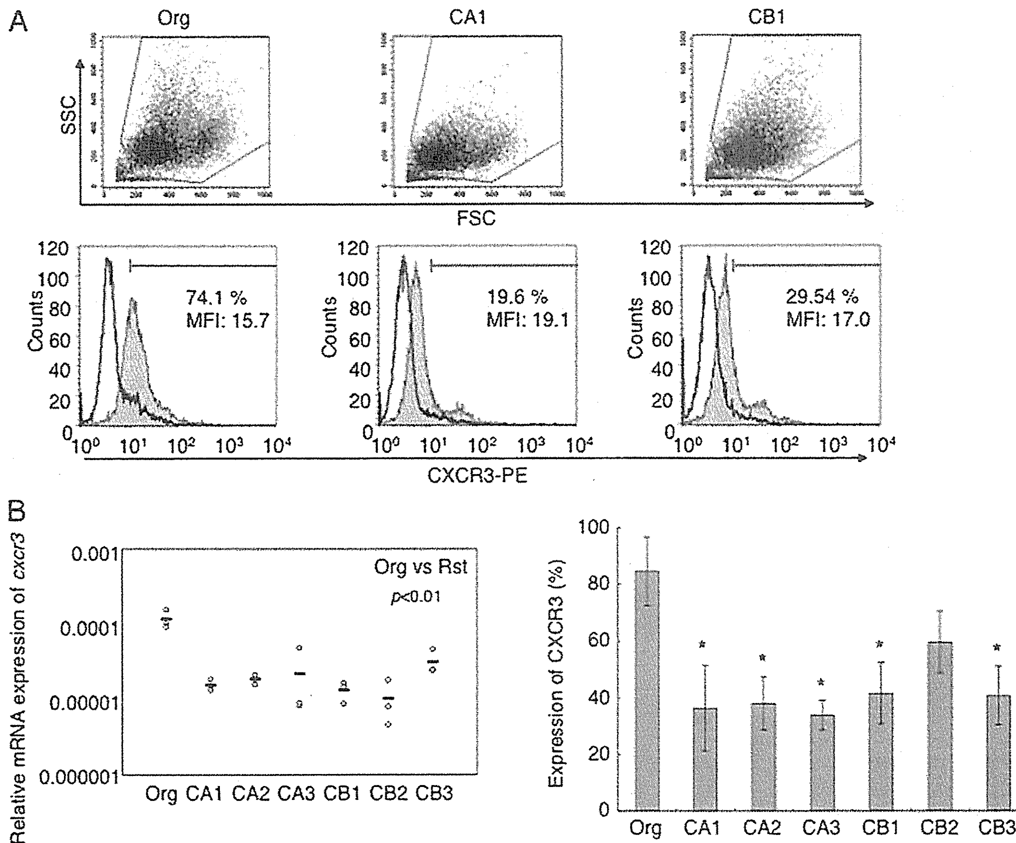

Figure 6. Chronic exposure to chrysotile inhibits the expression of CXCR3 in MT-2Rsts cells. (*A*) Representative FACS profiles of cell-surface CXCR3 expression on MT-2Org, CA1, and CB1. Living cells were gated, based on forward scatter (FSC) and side scatter (SSC) (*upper dot plot*). Gated cells were analyzed for the expression of CXCR3 (*lower histogram*). Peaks are shown in unstained control samples (*solid lines*) and stained samples (*gray peaks*). Percentages of CXCR3-positive cells and the mean fluorescence intensity (MFI) of gated cells are indicated in the histogram. (*B*) Total RNA was isolated, and the relative mRNA expression of *CXCR3* was estimated by real-time RT-PCR (*left*). Graph at *right* depicts the ratios of cell-surface CXCR3-positive cells in MT-2Org and MT-2Rsts. Results represent the mean ± SD of three independent experiments. *P* values were obtained using Dunnett's test. **P* < 0.01. ***P* < 0.05.

(known as Caplan's syndrome), systemic sclerosis, and antineutrophil cytoplasmic autoantibody–related vasculitis/nephritis (26–28). However, the most important complication in patients exposed to asbestos involves the occurrence of cancers, such as lung cancer and MM. In particular, MM is known to be caused by low-level and long-term exposures to asbestos (29–31).

We have been studying the mechanisms of dysregulation of autoimmunity caused by exposure to silica, and reported on alterations in Fas/CD95 and related molecules (32, 33), the activation of T cells by silica via the activation of antigen-presenting cells such as dendritic cells and monocyte/macrophage-lineage cells (34), and a reduction of regulatory T-cell function in the peripheral $CD4^+CD25^+$ fraction (35). On the other hand, asbestos is a mineral silicate that contains magnesium, iron, and calcium, with a core of SiO_2 (36, 37). Thus, asbestos may affect human immunocompetent cells because silica can modify human immunity (32–35). In view of these facts, if we think about the medical complications of a population exposed to silica or asbestos, patients may exhibit a reduced antitumor immune function because of developing cancers possessing a long-term latent phase (20–50 years) after an initial exposure to asbestos (29–31).

Therefore, we previously investigated the effects of asbestos on NK cells, and reported impairment in the cytotoxicity and expression of NK cell–activating receptor NKp46 and a decrease in the phosphorylation of the extracellular signal–regulated kinase signaling molecule in NK cells exposed to asbestos (11, 12). We also studied the effects of asbestos in relation to $CD8^+$ cytotoxic T cells, and found impairment in the differentiation and proliferation of these cells, the details of which will be reported in the future.

In regard to $CD4^+$ T cells, we established an *in vitro* cell line model of low-level and continuous exposure to asbestos (17, 18). MT-2 cells (15, 16) were chosen and underwent an initial screening for growth inhibition by culturing with asbestos to detect sensitivity to asbestos-induced apoptosis, because cell lines derived from leukemia and lymphoma may already possess alterations in many cellular and molecular events due to transformation. Moreover, chrysotile was initially used to analyze the immunologic effects of asbestos, because this fiber is used widely throughout the world.

First, we reported that high-dose and transient exposure induced apoptosis in MT-2 cells, caused by the production of ROS, the activation of proapoptotic c-Jun N-terminal kinase and p38 signaling molecules in the mitogen-activated protein kinase pathway, and the activation of the mitochondrial apoptotic pathway, as shown in Figure 1 (18). These findings were also evident when CA including 2% fibrous anthophyllite was used for exposure, as described in alveolar epithelial and pleural mesothelial cells (5–10). Next, we established a subline exposed to long-term and low-level CB (17). This subline showed the acquisition of resistance to asbestos-induced apoptosis through an activation of Src-family kinases, the up-regulation of IL-10 production, the activation of STAT3, and the up-regulation of Bcl-2, as shown in Figure 1 (17). Furthermore, the expression of *Bcl-2* in $CD4^+$ T cells from patients with MM was significantly up-regulated compared with that in healthy donors (17). However, because we ran only one trial to establish the low-level and continuous exposure model, we cannot confirm whether the findings in this subline represent general responses.

Therefore, we established five other independent sublines involving long-term and low-level exposure to chrysotile, because the other altered molecules should be identified for a better understanding of the asbestos-induced reduction of antitumor immune function. As shown in Figures 2 and 7A, all

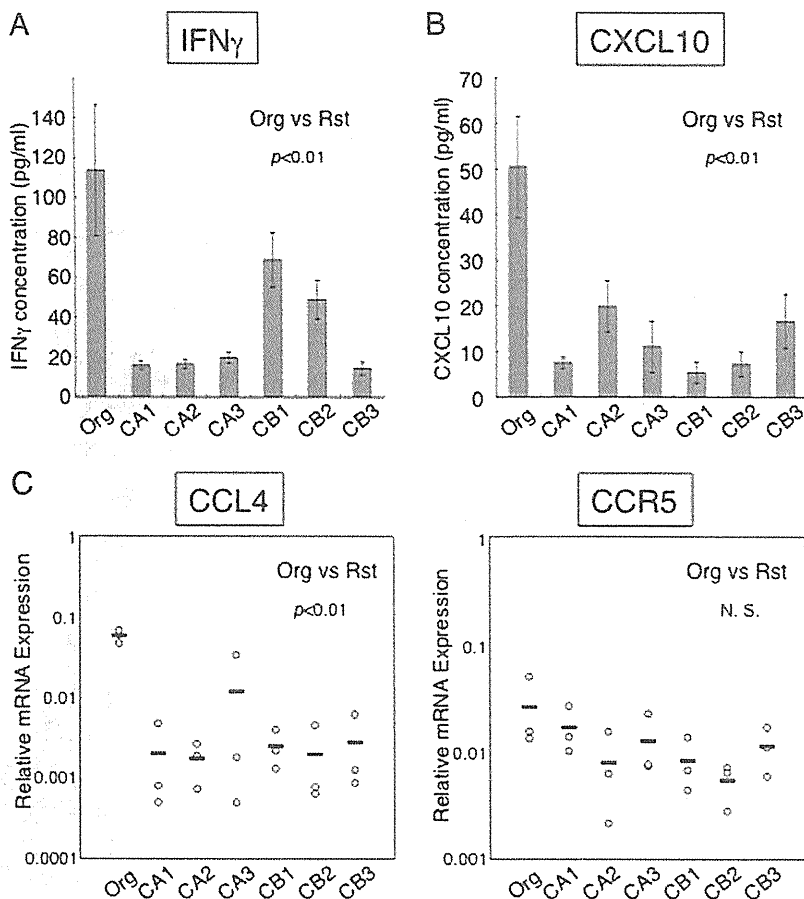

Figure 7. Continuous exposure to chrysotile decreases Th1-type cytokine IFN-γ and chemokine CXCL10/IP10 production in MT-2Rsts cells. (*A, B*) MT-2Org and MT-2Rsts cells were cultured for 72 hours. Culture supernatants were then collected and assessed for IFN-γ and CXCL10/IP10 production by ELISA. (*C*) The mRNA expressions of the Th1-type chemokine CCL4/MIP-1β and the receptor CCR5 were estimated using real-time RT-PCR. Results represent the mean ± SD of three independent experiments. *P* values were obtained using Dunnett's test. *$P < 0.01$. **$P < 0.05$.

six sublines, including the initial subline (CB1), exhibited a resistance to asbestos-induced apoptosis and a reduction of IFN-γ production, in a manner similar to that shown in previous studies (17). These findings indicate that the cellular and molecular alterations found in these sublines can be regarded as the universal immunologic effects of asbestos in T cells, although these findings should be confirmed using freshly isolated lymphocytes from both healthy donors and patients with MM exposed to asbestos.

An exhaustive analysis using DNA microarray, pathway, and network analyses identified the suppression of the Thl-type IFN-γ signaling pathway and CXCR3 expression. These alterations were confirmed by the decreased production of IFN-γ and decreased cell-surface expression of CXCR3 in all cell lines. IFN-γ is an antitumor cytokine, and it is used for the treatment of various cancers to enhance the antitumor activity of T cells, NK cells, and natural killer T cells (38, 39). In addition, the chemokine receptor CXCR3 is a G-protein–coupled seven-transmembrane receptor expressed on various lymphocytes, including T cells, B cells, and NK cells, and it binds to IFN-γ–inducible chemokines such as CXCL9/MIG, CXCL10/IP10, and CXCL11/I-TAC that recruit leukocytes to inflammatory sites such as tumors (40). In the case of $CD4^+$ T cells, CXCR3 is preferentially expressed on IFN-γ–producing Thl/effector T cells. Our previous study showed that original MT-2 cells exhibit a high-level production of inflammatory cytokine IFN-γ, TNF-α, and IL-6, whereas sublines produce an anti-inflammatory cytokine IL-10 at a high concentration (17), suggesting that the Thl/effector T-cell–like characteristics of MT-2Org cells may easily be suppressed by long-term and low-level exposures to chrysotile, although the mRNA expression of Thl-type CCR5 (41) was not inhibited significantly (Figure 7C). Moreover, all six sublines showed a down-regulation of Thl-type chemokine CXCL10/IP10 and CCL4/MIP-1β. Generally, both CXCL10/IP10 and CCL4/MIP-1β are secreted by activated T cells, and contribute to the attraction of Thl/effector T cells (41, 42). Therefore, the suppression of Thl-type molecules such as CXCR3, IFN-γ, CXCL10/IP10, and CCL4/MIP-1β in sublines continuously exposed to chrysotile can be considered evidence of asbestos-induced cellular and molecular alterations in immunocompetent cells. Exposure to asbestos seems to modify antitumor immune function and local (pulmonary) inflammatory reactions because of changes in the expression and production levels of cytokines, chemokines, and chemokine receptors in immune competent cells.

These findings may provide an explanation for the rapid progression of asbestos-related cancers, although further research is needed to confirm whether these alterations in cell-line models arise in freshly isolated human lymphocytes derived from healthy donors and patients with PP or MM.

Author Disclosure: None of the authors has a financial relationship with a commercial entity that has an interest in the subject of this manuscript.

Acknowledgments: We thank Tamayo Hatayama, Minako Kato, Naomi Miyahara, Shoko Yamamoto, Misao Kuroki, Keiko Kimura, Yoshiko Yamashita, and Tomoko Sueishi for technical assistance.

References

1. Pan XL, Day HW, Wang W, Beckett LA, Schenker MB. Residential proximity to naturally occurring asbestos and mesothelioma risk in California. *Am J Respir Crit Care Med* 2005;172:1019–1025.
2. Cugell DW, Kamp DW. Asbestos and the pleura: a review. *Chest* 2004; 125:1103–1117.
3. Miserocchi G, Sancini G, Mantegazza F, Chiappino G. Translocation pathways for inhaled asbestos fibers. *Environ Health* 2008;7:4.

4. Murayama T, Takahashi K, Natori Y, Kurumatani N. Estimation of future mortality from pleural malignant mesothelioma in Japan based on an age-cohort model. *Am J Ind Med* 2006;49:1–7.
5. Upadhyay D, Kamp DW. Asbestos-induced pulmonary toxicity: role of DNA damage and apoptosis. *Exp Biol Med (Maywood)* 2003;228: 650–659.
6. Panduri V, Surapureddi S, Soberanes S, Weitzman SA, Chandel N, Kamp DW. P53 mediates amosite asbestos–induced alveolar epithelial cell mitochondria–regulated apoptosis. *Am J Respir Cell Mol Biol* 2006;34:443–452.
7. Upadhyay D, Panduri V, Kamp DW. Fibroblast growth factor–10 prevents asbestos-induced alveolar epithelial cell apoptosis by a mitogen-activated protein kinase–dependent mechanism. *Am J Respir Cell Mol Biol* 2005;32:232–238.
8. Mossman BT. Introduction to serial reviews on the role of reactive oxygen and nitrogen species (ROS/RNS) in lung injury and diseases. *Free Radic Biol Med* 2003;34:1115–1116.
9. Kamp DW, Panduri V, Weitzman SA, Chandel N. Asbestos-induced alveolar epithelial cell apoptosis: role of mitochondrial dysfunction caused by iron-derived free radicals. *Mol Cell Biochem* 2002;234–235: 153–160.
10. Jiang L, Nagai H, Ohara H, Hara S, Tachibana M, Hirano S, Shinohara Y, Kohyama N, Akatsuka S, Toyokuni S. Characteristics and modifying factors of asbestos-induced oxidative DNA damage. *Cancer Sci* 2008;99:2142–2151.
11. Nishimura Y, Miura Y, Maeda M, Kumagai N, Murakami S, Hayashi H, Fukuoka K, Nakano T, Otsuki T. Impairment in cytotoxicity and expression of NK cell-activating receptors on human NK cells following exposure to asbestos fibers. *Int J Immunopathol Pharmacol* 2009;22:579–590.
12. Nishimura Y, Maeda M, Kumagai N, Hayashi H, Miura Y, Otsuki T. Decrease in phosphorylation of ERK following decreased expression of NK cell–activating receptors in human NK cell line exposed to asbestos. *Int J Immunopathol Pharmacol* 2009;22:879–888.
13. Ueki A, Yamaguchi M, Ueki H, Watanabe Y, Ohsawa G, Kinugawa K, Kawakami Y, Hyodoh F. Polyclonal human T-cell activation by silicate *in vitro*. *Immunology* 1994;82:332–335.
14. Aikoh T, Tomokuni A, Matsukii T, Hyodoh F, Ueki H, Otsuki T, Ueki A. Activation-induced cell death in human peripheral blood lymphocytes after stimulation with silicate *in vitro*. *Int J Oncol* 1998;12:1355–1359.
15. Miyoshi I, Kubonishi I, Yoshimoto S, Shiraishi Y. A T-cell line derived from normal human cord leukocytes by co-culturing with human leukemic T-cells. *Gann* 1981;72:978–981.
16. Miyoshi I, Kubonishi I, Yoshimoto S, Akagi T, Ohtsuki Y, Shiraishi Y, Nagata K, Hinuma Y. Type C virus particles in a cord T-cell line derived by co-cultivating normal human cord leukocytes and human leukaemic T cells. *Nature* 1981;294:770–771.
17. Miura Y, Nishimura Y, Katsuyama H, Maeda M, Hayashi H, Dong M, Hyodoh F, Tomita M, Matsuo Y, Uesaka A, *et al.* Involvement of IL-10 and Bcl-2 in resistance against an asbestos-induced apoptosis of T cells. *Apoptosis* 2006;11:1825–1835.
18. Hyodoh F, Takata-Tomokuni A, Miura Y, Sakaguchi H, Hatayama T, Hatada S, Katsuyama H, Matsuo Y, Otsuki T. Inhibitory effects of anti-oxidants on apoptosis of a human polyclonal T-cell line, MT-2, induced by an asbestos, chrysotile-A. *Scand J Immunol* 2005;61:442–448.
19. Maeda M, Miura Y, Nishimura Y, Murakami S, Hayashi H, Kumagai N, Hatayama T, Katoh M, Miyahara N, Yamamoto S, *et al.* Immunological changes in mesothelioma patients and their experimental detection. *Clin Med Insights Circ Respir Pulmon Med* 2008;2:11–17.
20. Nishimura Y, Miura Y, Maeda M, Hayashi H, Dong M, Katsuyama H, Tomita M, Hyodoh F, Kusaka M, Uesaka A, *et al.* Expression of the T cell receptor Vbeta repertoire in a human T cell resistant to asbestos-induced apoptosis and peripheral blood T cells from patients with silica and asbestos-related diseases. *Int J Immunopathol Pharmacol* 2006;19:795–805.
21. Kohyama N, Shinohara Y, Suzuki Y. Mineral phases and some reexamined characteristics of the International Union against Cancer standard asbestos samples. *Am J Ind Med* 1996;30:515–528.
22. Luster AD, Leder P. IP-10, a -C-X-C- chemokine, elicits a potent thymus-dependent antitumor response *in vivo*. *J Exp Med* 1993;178: 1057–1065.
23. Abraham JL. Recent advances in pneumoconiosis: the pathologist's role in etiologic diagnosis. *Monogr Pathol* 1978;19:96–137.
24. Vallyathan NV, Green FH, Craighead JE. Recent advances in the study of mineral pneumoconiosis. *Pathol Annu* 1980;15:77–104.
25. Begin R, Cantin A, Masse S. Recent advances in the pathogenesis and clinical assessment of mineral dust pneumoconioses: asbestosis, silicosis and coal pneumoconiosis. *Eur Respir J* 1989;2:988–1001.
26. Scheule RK, Holian A. Immunologic aspects of pneumoconiosis. *Exp Lung Res* 1991;17:661–685.
27. Uber CL, McReynolds RA. Immunotoxicology of silica. *Crit Rev Toxicol* 1982;10:303–319.
28. Steenland K, Goldsmith DF. Silica exposure and autoimmune diseases. *Am J Ind Med* 1995;28:603–608.
29. Kannerstein M, Churg J, McCaughey WT. Asbestos and mesothelioma: a review. *Pathol Annu* 1978;13:81–129.
30. Kannerstein M, Churg J, McCaughey E, Selikoff IJ. Pathogenic effects of asbestos. *Arch Pathol Lab Med* 1977;101:623–628.
31. Craighead JE, Mossman BT. The pathogenesis of asbestos-associated diseases. *N Engl J Med* 1982;306:1446–1455.
32. Otsuki T, Miura Y, Nishimura Y, Hyodoh F, Takata A, Kusaka M, Katsuyama H, Tomita M, Ueki A, Kishimoto T. Alterations of Fas and Fas-related molecules in patients with silicosis. *Exp Biol Med (Maywood)* 2006;231:522–533.
33. Otsuki T, Maeda M, Murakami S, Hayashi H, Miura Y, Kusaka M, Nakano T, Fukuoka K, Kishimoto T, Hyodoh F, *et al.* Immunological effects of silica and asbestos. *Cell Mol Immunol* 2007;4:261–268.
34. Wu P, Hyodoh F, Hatayama T, Sakaguchi H, Hatada S, Miura Y, Takata-Tomokuni A, Katsuyama H, Otsuki T. Induction of CD69 antigen expression in peripheral blood mononuclear cells on exposure to silica, but not by asbestos/chrysotile-A. *Immunol Lett* 2005;98:145–152.
35. Wu P, Miura Y, Hyodoh F, Nishimura Y, Hatayama T, Hatada S, Sakaguchi H, Kusaka M, Katsuyama H, Tomita M, *et al.* Reduced function of $CD4^{+}25^{+}$ regulatory T cell fraction in silicosis patients. *Int J Immunopathol Pharmacol* 2006;19:357–368.
36. Pooley FD. Mineralogy of asbestos: the physical and chemical properties of the dusts they form. *Semin Oncol* 1981;8:243–249.
37. Stephens M, Gibbs AR, Pooley FD, Wagner JC. Asbestos induced diffuse pleural fibrosis: pathology and mineralogy. *Thorax* 1987;42: 583–588.
38. Rudge G, Barrett SP, Scott B, van Driel IR. Infiltration of a mesothelioma by IFN-gamma–producing cells and tumor rejection after depletion of regulatory T cells. *J Immunol* 2007;178:4089–4096.
39. Miller CH, Maher SG, Young HA. Clinical use of interferon-gamma. *Ann N Y Acad Sci* 2009;1182:69–79.
40. Rotondi M, Chiovato L, Romagnani S, Serio M, Romagnani P. Role of chemokines in endocrine autoimmune diseases. *Endocr Rev* 2007;28: 492–520.
41. Luther SA, Cyster JG. Chemokines as regulators of T cell differentiation. *Nat Immunol* 2001;2:102–107.
42. Loetscher M, Loetscher P, Brass N, Meese E, Moser B. Lymphocyte-specific chemokine receptor CXCR3: regulation, chemokine binding and gene localization. *Eur J Immunol* 1998;28:3696–3705.

Clinical Cancer Research

Epigenetic Silencing of MicroRNA-34b/c Plays an Important Role in the Pathogenesis of Malignant Pleural Mesothelioma

Takafumi Kubo[1], Shinichi Toyooka[1], Kazunori Tsukuda[1], Masakiyo Sakaguchi[2], Takuya Fukazawa[3], Junichi Soh[1], Hiroaki Asano[1], Tsuyoshi Ueno[1], Takayuki Muraoka[1], Hiromasa Yamamoto[1], Yasutomo Nasu[4], Takumi Kishimoto[6], Harvey I. Pass[7], Hideki Matsui[5], Nam-ho Huh[2], and Shinichiro Miyoshi[1]

Abstract

Purpose: Malignant pleural mesothelioma (MPM) is an aggressive tumor with a dismal prognosis. Unlike other malignancies, *TP53* mutations are rare in MPM. Recent studies have showed that altered expression of microRNA (miRNA) is observed in human malignant tumors. In this study, we investigated the alterations of miR-34s, a direct transcriptional target of *TP53*, and the role of miR-34s on the pathogenesis of MPM.

Experimental Design: Aberrant methylation and expression of miR-34s were examined in MPM cell lines and tumors. miR-34b/c was transfected to MPM cells to estimate the protein expression, cell proliferation, invasion, and cell cycle.

Results: Aberrant methylation was present in 2 (33.3%) of 6 MPM cell lines and 13 (27.7%) of 47 tumors in miR-34a and in all 6 MPM cell lines (100%) and 40 (85.1%) of 47 tumors in miR-34b/c. Expression of miR-34a and 34b/c in all methylated cell lines was reduced and restored with 5-aza-2′-deoxycytidine treatment. Because epigenetic silencing was the major event in miR-34b/c, we investigated the functional role of miR-34b/c in MPM. miR-34b/c–transfected MPM cells with physiologic miR-34b/c expression exhibited antiproliferation with G_1 cell cycle arrest and suppression of migration, invasion, and motility. The forced overexpression of miR-34b/c, but not p53, showed a significant antitumor effect with the induction of apoptosis in MPM cells.

Conclusions: We show that the epigenetic silencing of miR-34b/c by methylation is a crucial alteration and plays an important role in the tumorigenesis of MPM, suggesting potential therapeutic options for MPM. *Clin Cancer Res; 17(15); 4965–74. ©2011 AACR.*

Introduction

Malignant pleural mesothelioma (MPM) is a neoplasm with highly invasive and aggressive clinical features (1). Exposure to asbestos is strongly associated with the etiology of MPM. A curative modality such as radiotherapy, conventional chemotherapy, or molecular targeting therapy has not yet been established for advanced MPM and the development of new treatments is needed (2). An understanding of molecular pathogenesis is crucial for developing new therapeutic strategies. However, much less information about molecular alterations in MPM is available than for other neoplasms. Previous studies have revealed that the genetic alterations of MPM are quite different from that of other neoplasms. One of the unique molecular features of MPM is that mutations and deletions of the *TP53* gene are rare (3, 4), even though MPM generally exhibits cell cycle alterations and antiapoptosis, which suggests functional p53 deficiency (5). Considering these observations, uncovering the molecular pathogenesis of MPM is likely to provide useful information.

MicroRNAs (miRNA) are a group of noncoding small RNAs that generally regulate their target mRNAs by post-transcriptional repression (6). In the recent half decade, intensive research about the role of miRNAs in human malignant tumors has been conducted because of the ability of individual miRNAs to regulate multiple genes implicated in multiple pathways (7). Similar to encoding genes, some miRNAs have been classified as oncogenic or

Authors' Affiliations: Departments of [1]Cancer and Thoracic Surgery, [2]Cell Biology, [3]Gastroenterological Surgery, Transplant, and Surgical oncology, [4]Urology, and [5]Cellular Physiology, Okayama University Graduate School of Medicine, Dentistry and Pharmaceutical Sciences; [6]Department of Internal Medicine, Okayama Rosai Hospital, Okayama, Japan; and [7]Division of Thoracic Surgery, Department of Cardiothoracic Surgery, NYU Langone Medical Center, New York

Note: Supplementary data for this article are available at Clinical Cancer Research Online (http://clincancerres.aacrjournals.org/).

Corresponding Author: Shinichi Toyooka, Department of Cancer and Thoracic Surgery, Okayama University Graduate School of Medicine, Dentistry and Pharmaceutical Sciences, 2-5-1 Shikata-cho, Kita-ku, Okayama 700-8558, Japan. Phone: 81-86-235-7265; Fax: 81-86-235-7269; E-mail: toyooka@md.okayama-u.ac.jp

doi: 10.1158/1078-0432.CCR-10-3040

©2011 American Association for Cancer Research.

Translational Relevance

Malignant pleural mesothelioma (MPM) is an aggressive tumor with a dismal prognosis. Unlike other malignancies, mutations of *TP53* are rare in MPM. Here, we found that the methylation of miR-34b/c, direct transcriptional targets of the p53, was often present resulting in reduced expression in MPM. The miR-34b/c–transfected MPM cells showed antiproliferation with G_1 arrest and inhibition of migration, invasion, and motility. Overexpression of miR-34b/c, but not p53, showed significant antitumor effect by apoptosis in MPM cells. Our results show that epigenetic silencing of miR-34b/c plays a pivotal role in pathogenesis of MPM and suggest that miR-34b/c can be a potential therapeutic target for MPM.

tumor-suppressive miRNAs according to their effects on cellular transformation (8). Among the tumor-suppressive miRNAs, the miR-34s, which have p53 response elements in their 5′ flanking regions, have recently been investigated (9–11). The members of the miR-34 family are composed of 3 miRNAs, miR-34a, miR-34b, and miR-34c, whose target genes are considered to be similar but with some notable differences (9). miR-34a is located on chromosome 1q36.22, whereas miR-34b and miR-34c (miR-34b/c) are located on chromosome 11q23 and are generated by the processing of a single transcript (9). The miR-34 family members are direct transcriptional targets of p53 and constitute a part of p53 tumor suppressor network regulating cell cycle arrest, apoptosis, and senescence (9, 12). Indeed, miR-34s were downregulated in *TP53*-null or *TP53*-mutant cells (9, 11).

Aberrant methylation of CpG islands located in the promoter region has been shown to be associated with the transcriptional inactivation of tumor suppressor genes in various human malignancies including MPM (13, 14). Similar to tumor suppressor genes, miRNAs may be downregulated in cancers through epigenetic mechanisms (15–17). Epigenetic silencing of miR-34s has been documented in several human malignancies including colorectal cancers (10, 17, 18). Recent studies have indicated the aberrant expressions of miRNAs in MPM, suggesting their roles in carcinogenesis (19–21). Taken together, these previous findings led us to investigate the molecular pathogenetic significance of miR-34s in MPM.

In this study, we examined the methylation and expression status of miR-34s in MPM and found that epigenetic silencing of miR-34b/c by DNA methylation occurred quite frequently in MPM. On the basis of this finding, the cellular biological effects of miR-34b/c were examined in MPM to elucidate the role of miR-34b/c in the pathogenesis of MPM and to explore the possibility of the therapeutic potential of miR-34b/c for MPM.

Materials and Methods

Clinical samples and cell lines

Surgically resected specimens of 47 MPMs were obtained from Okayama University Hospital, Okayama, Japan (5 cases), and from Karmanos Cancer Institute, Detroit, MI (42 cases). Written informed consents were obtained from all patients at 2 collection sites. The histologic subtypes of primary MPM consisted of 32 epithelial, 10 biphasic, 4 sarcomatoid, and 1 lymphohistiocytic variant types. Ten nonneoplastic pleura from lung cancer patients were obtained from surgically resected pulmonary specimens and were used for the methylation assay. In addition, 2 nonmalignant mesothelial primary cultures (mesothelial cells) were established from pleural effusions that arose in patients free of cancer, as described in our previous report (22), and these cells were used as controls. All the tissues were frozen in liquid nitrogen immediately after surgery and stored at −80°C. Six MPM cell lines [NCI-H28 (H28), NCI-H290 (H290), NCI-H2052 (H2052), NCI-H2452 (H2452), HP1, and MSTO-211H], a lung cancer cell line [NCI-H125 (H125)], and 1 human bronchial epithelial cell line (HBEC 5KT) were used in this study. Six cell lines (H28, H290, H2052, H2452, H125, and HBEC 5KT) were kind gifts from Dr. Adi F. Gazdar (Hamon Center for Therapeutic Oncology Research and Department of Pathology, University of Texas Southwestern Medical Center at Dallas, Dallas, TX). These cell lines were proven to have individual genetic origins by the PowerPlex 1.2 System (Promega) at University of Texas Southwestern Medical Center at Dallas (23). The HP1 cell line was established by H.I. Pass. MSTO-211H was obtained from American Type Culture Collection. The cells were maintained in RPMI 1640 medium (Sigma Chemical Co.) supplemented with 10% FBS and incubated in 5% CO_2 except for HBEC 5KT, which was maintained in Keratinocyte-SFM (Invitrogen) with bovine pituitary extract and human recombinant epidermal growth factor (24). The cell lines were treated with 5-aza-2′-deoxycytidine (DAC; Sigma-Aldrich Co.) at a concentration of 5 μmol/L for 6 days to restore the gene expression that was reduced by methylation.

Methylation-specific PCR assay and bisulfite DNA sequencing

Genomic DNA was extracted from cell lines and tissues, and DNA was subjected to bisulfite treatment. The methylation status of miR-34s was determined by methylation-specific PCR (MSP) assay and bisulfite DNA sequencing as previously reported (17, 18, 25). The extent of miR-34b/c methylation was determined by real-time quantitative MSP (q-MSP) assay using Power SYBR Green PCR Master Mix (Applied Biosystems). Further details are provided in Supplementary Methods.

Evaluation of miR-34s expression using quantitative reverse transcription-PCR

miRNA was isolated from cell lines and tissue specimens and the reverse transcription reaction was carried out. The

quantitative reverse transcription PCR (RT-PCR) for miR-34a, miR-34b, and miR-34c was carried out with normalization of expression value as described in Supplementary Methods.

Plasmid construction, gene transfection, and colony formation assay

The miR-34b/c or scramble sequence fragment as control was subcloned into pSilencer 4.1-CMV neo Plasmid Vector (Ambion; refs. 17, 18, 25). Four micrograms of constructed plasmids was introduced into MPM cells using Lipofectamine 2000 Reagent (Invitrogen). For experiments of transient transfection, cells were collected 72 hours after transfection. To establish stable transfectants, selection of the cells was started 48 hours after transfection in 6-well plates with G418 (Gibco) antibiotics. Resistant clones were cloned by ring isolation after 3 weeks of selection. *In vitro* cell proliferation was tested by liquid colony formation assay (details in Supplementary Methods).

Western blot analysis

Preparation of total cell lysates and Western blot analysis were done as described in Supplementary Methods. We selected 7 molecules (c-MET, CDK4, CDK6, CCND1, CCNE2, Bcl-2, c-MYC, and E2F3) that had been reported as primary targets of miR-34s (9, 11, 26).

Flow cytometric analysis

Cells were harvested and resuspended in PBS containing 0.2% Triton X-100 and 1 mg/mL RNase for 5 minutes at room temperature and then stained with propidium iodide at 50 μg/mL to determine subdiploid DNA content using a FACScan. Doublets, cell debris, and fixation artifacts were gated out, and cell cycle analysis was done using CellQuest version 3.3 software.

Cell migration, invasion, and motility assays

The cell migration and invasion ability were estimated using a Boyden chamber assay with filter inserts (pore size: 8 μm) in 6-well dishes (BD Biosciences Discovery Labware). The motility of MPM cells was estimated using time lapse video microscopy using a Keyence BZ-8000 (Keyence). Further details are provided in Supplementary Methods.

Recombinant adenoviral vector construction

Ad-miR-34b/c driven by cytomegalovirus (CMV) promoter (Ad-miR-34b/c) was generated by homologous recombination and plaque purified (27). Adenoviral vector expressing p53 driven by CMV promoter (Ad-p53) and adenoviral vector expressing luciferase driven by CMV promoter (Ad-Luc) were used as control vectors. The optimal multiplicity of infection (MOI) was determined by infecting each cell line with Ad-CMV/GFP and assessing the expression of green fluorescent protein (GFP) by flow cytometric analysis. H28, H290, and H2052 MPM cell lines were infected with the adenoviral vectors at an MOI of 200 plaque-forming units (pfu) per cell. All other cancer cell lines were infected at a MOI of 50 pfu per cell.

MTS assay for cell viability in adenoviral-infected cells

Cells were plated in 96-well plates at a density of 1.0×10^3 cells per well 24 hours before infections and treated with PBS, Ad-Luc, Ad-p53, or Ad-miR-34b/c. Cell viability was evaluated at 0, 1, 2, 3, and 4 days following the adenoviral infection by MTS assay with CellTiter 96 AQueous One Solution Reagent (Promega).

Statistical analysis

Data were represented as mean ± SD. Mann–Whitney *U* test was used to compare data between 2 groups. $P < 0.05$ was considered as being statistically significant.

Results

Methylation and expression status of miR-34s in MPM and other cancers

The methylation status of miR-34s was determined by MSP assay and bisulfite DNA sequencing as previously reported (17, 18, 25). Representative examples of MSP assays are shown in Figure 1A and B. In the 6 MPM cell lines examined, miR-34a was methylated in 2 (33.3%) cell lines (H28 and H290) and miR-34b/c was methylated in all the 6 cell lines (100%). In 47 MPM tumors, miR-34a methylation was present in 13 (27.7%) cases: 10 (31.2%) of the 32 epithelial-type tumors, 1 (10%) of the 10 biphasic-type tumors, 2 (50%) of the 4 sarcomatoid-type tumors, and none of the 1 lymphohistiocytic variant–type tumor. miR-34b/c methylation was present in 40 (85.1%) cases: 29 (90.6%) epithelial-type tumors, 7 (70%) biphasic-type tumors, 3 (75%) sarcomatoid-type tumors, and 1 (100%) lymphohistiocytic variant–type tumors. No methylation was found in 10 nonneoplastic pleura specimens and 2 nonmalignant mesothelial cells. All the MPMs that had miR-34a methylation also had miR-34b/c methylation. We quantified the extent of methylation of miR-34b/c using q-MSP assay in 3 MPM cell lines. NCI-H2052 and NCI-H290 showed 2 ± 0.2-fold and 5 ± 0.6-fold increase of the extent of miR-34b/c methylation compared with NCI-H28 by quantitative MSP assay, respectively (not shown as a table or a figure). We also evaluated the degree of methylation of miR-34b/c using subcloning technique of bisulfate sequencing, and heavy methylation at the CpG sites in the 5′ flanking region of miR-34b/c was observed (Fig. 1C). Of note, the percentage of methylated CpG sites that was evaluated by subcloning technique was higher in NCI-H2052 (93.9%) and NCI-H290 (97.7%) than in NCI-H28 (74.2%; Fig. 1C). In contrast, methylation at the CpG sites was rarely observed in nonmalignant mesothelial cells.

The expression of miR-34a, miR-34b, and miR-34c in MPM cell lines and primary tumors was examined using quantitative RT-PCR. Because the expression levels of the 2 nonmalignant mesothelial cells were similar, we mixed them and used them as standards for expression of nonmalignant mesothelial cells. The expression value of miR-34s in the cells was defined as the ratio of the expression in individual cell lines to that of nonmalignant mesothelial cells and was arbitrarily assigned a value of 100. We

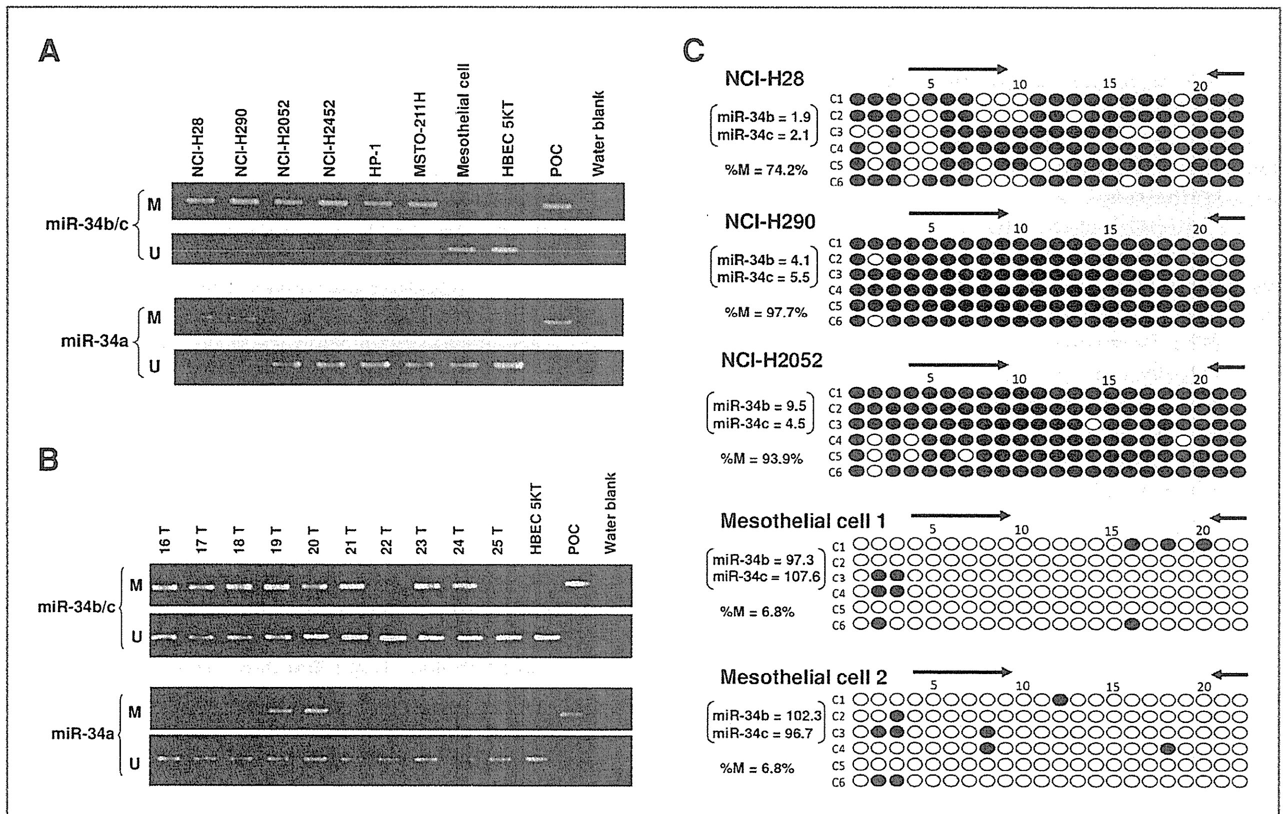

Figure 1. Methylation status of miR-34a and miR-34b/c in MPMs. A and B, representative examples of conventional MSP for miR-34a and miR-34b/c in MPM cells (A) and primary tumors (B). The unmethylated form of miR-34s was always found in primary tumors that had some contamination with normal cells. M, methylated; U, unmethylated; POC, positive control (SssI-treated DNA). C, methylation status of individual cloned DNA fragments of 3 MPM cell lines and 2 nonmalignant mesothelial cells is shown. Each row represents 1 sequenced allele. Each circle represents a CpG dinucleotide (closed circle, methylated; opened circle, unmethylated). Clonal numbers are indicated by prefix C to the left. The numbers at the top indicate the CpG dinucleotide in the amplicon (5′ to 3′). The positions of CpG dinucleotides for MSP primers reported previously are indicated by horizontal arrows. The values in parentheses were expression values of miR-34b/c in each cell line compared with the nonmalignant mesothelial cells whose miR-34b/c expression was defined as 100. %M, the rate of methylated CpG dinucleotides.

arbitrarily considered the cell lines whose miR-34s expression values were less than 10 as being MPM cell lines with reduced expression. These expression values were reduced in all the methylated MPM cell lines and were not reduced in the unmethylated MPM cell lines. The expression values of cell lines are shown in Table 1. To confirm the results

Table 1. The expression and methylation status of miR-34s in cell lines

Cell lines	Histology	Methylation status		miR expression value		
		miR-34a	miR-34b/c	miR-34a	miR-34b	miR-34c
NCI-H28	MPM (sarcomatoid)	M	M	0.5	1.9	2.1
NCI-H290	MPM (epithelial)	M	M	0.9	4.1	5.5
NCI-H2052	MPM (epithelial)	U	M	49.3	9.5	4.5
NCI-H2452	MPM (biphasic)	U	M	99.9	8	9.1
HP-1	MPM (biphasic)	U	M	11.7	5.8	0.8
MSTO-211H	MPM (biphasic)	U	M	37.7	0.4	1.5
NCI-H125	Lung cancer (adenosquamous carcinoma)	M/U	U	1.9	21.5	13
HBEC 5KT	–	U	U	323	695	358
Mesothelial cells		U	U	100	100	100

NOTE: miR-34s expression values are relative expression values compared with those of nonmalignant mesothelial cells, which are defined as 100.

Table 2. Expression values of miR-34s in MPM cells with miR-34b/c transfection

Cell lines		miR expression value		
		miR-34a	miR-34b	miR-34c
A. Plasmid stable transfectants				
NCI-H28	p-Scramble	0.7	1.8	2.5
	p-miR-34b/c	0.8	131	94.7
NCI-H290	p-Scramble	1.4	3	5
	p-miR-34b/c	1.3	25.6	28.8
NCI-H2052	p-Scramble	47.8	9.3	4.5
	p-miR-34b/c	52.6	62.6	68.8
Mesothelial cell		100	100	100
B. Adenoviral-transfected cells				
NCI-H28	Ad-Luc	0.6	2.1	2.5
	Ad-miR-34b/c	0.9	1,470	6,540
NCI-H290	Ad-Luc	1.2	4.3	5.5
	Ad-miR-34b/c	1.1	501	2,170
NCI-H2052	Ad-Luc	50.1	10.5	5.2
	Ad-miR-34b/c	54.2	1,640	3,430
Mesothelial cell		100	100	100

obtained from cell lines, we assessed the relationship between methylation and expression status for miR-34b/c in primary tumors. We randomly chose 10 samples (different sets from the ones shown in Fig. 1B) and examined the expression of miR-34b and miR-34c. In the 10 samples tested, 2 samples were unmethylated and we set the expression of miR-34b/c in one of them as 100 and compared the other samples with it. Similar results were obtained in 10 clinical samples (Supplementary Table S3). We treated 6 MPM cell lines with DAC and found that the expression of the miR-34s was restored in the methylated MPM cell lines. The degree of upregulation in the expression of miR-34s after DAC treatment ranged from 4- to 80.9-fold in methylated genes (Supplementary Table S1).

Impact of miR-34b/c on cell proliferation

To screen for the antiproliferative effect of miR-34b/c, a colony formation assay was conducted with transient transfection. Four MPM cell lines (H28, H290, H2052, and H2452) were transiently transfected with miR-34b/c or a scrambled control. Colony formation was remarkably inhibited in 3 MPM cell lines with miR-34b/c transfection, compared with that in cells transfected with the scramble control (55% inhibition in H28, $P < 0.01$; 42% in H290, $P < 0.01$; and 64% in H2052, $P < 0.01$; Supplementary Fig. S1A and B). No colonies were formed in H2452 transfected with the scramble control or miR-34b/c (data not shown). Of note, although a colony formation assay after transient transfection showed antiproliferation in MPM cell lines, we found significant cell toxicity, probably caused by the transfection itself, in MPM cell lines transfected with scramble or miR-34b/c plasmid vectors. Thus, we established stable transfectants to investigate the various cellular effects of miR-34b/c on MPM.

Establishment of stable transfectants

We established stable transfectants with miR-34b/c and the scramble control in H28, H290, and H2052. The expression values of the miR-34b/c stable transfectants ranged from 25.6 to 131, shown in Table 2, part A. These values were not so different from that of nonmalignant mesothelial cells; therefore, the expression of miR-34b and miR-34c in the stable transfectants was considered to be within the physiologic range of nonmalignant mesothelial cells. A colony formation assay of stable transfectants confirmed that cell proliferation was significantly inhibited in MPM cells transfected with miR-34b/c, compared with that in cells transfected with the scramble control (Fig. 2A and B).

Protein expression and cell cycle analysis of stable transfectants

To examine the effect of miR-34b/c introduction, we focused on c-MET, CDK4, CDK6, CCND1, CCNE2, Bcl-2, c-MYC, and E2F3, which have been reported as putative targets of miR-34b/c (9, 25). Western blotting was carried out in MPM stable transfectants. Total and phosphorylated c-MET expression, in particular, was strongly downregulated in the 3 MPM cell lines examined. CDK4, CDK6, CCND1, CCNE2, c-MYC, and E2F3 tended to be downregulated by the miR-34b/c in cell lines in which native protein expression was present (Fig. 2C). There seemed to be no difference in Bcl-2 expression between the miR-34b/c and control transfectants. We chose p-c-MET and c-MYC as a representative and quantified the protein expression level

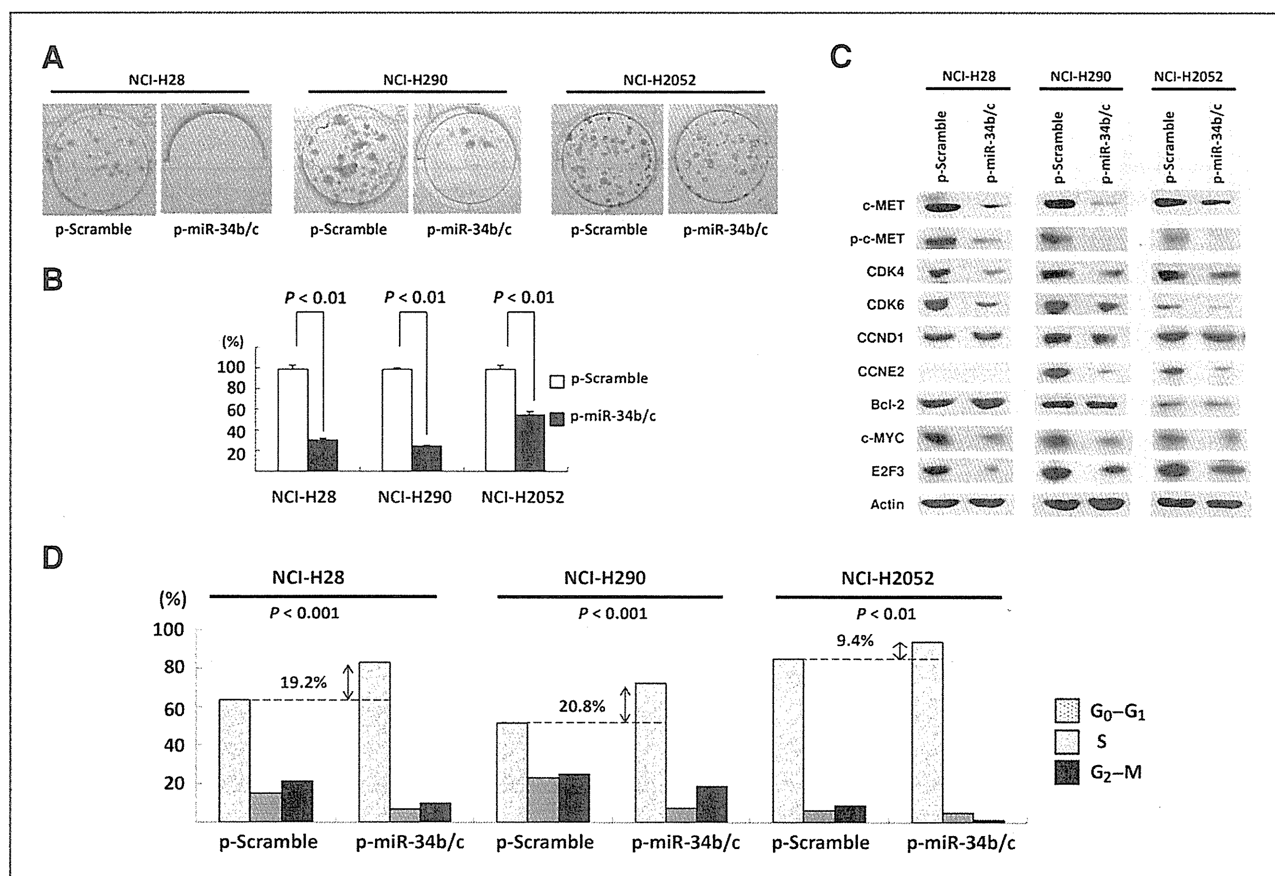

Figure 2. Colony formation assays of MPM cells stably transfected with miR-34b/c or control plasmid vectors. A, representative results from a colony formation assay. B, relative colony formation efficiencies. Shown are means of 3 replications; error bars represent SD. Protein expression profile (C) and cell cycles (D) of MPM stable miR-34b/c transfectants.

of them by densitometry analysis using NIH ImageJ software tentatively (Supplementary Fig. S7). Although there may not be much point in quantifying the protein expression obtained by Western blot, the results seem to be consistent with an effect by the miR-34b/c.

A cell cycle analysis was conducted for MPM stable miR-34b/c and control transfectants. All 3 MPM stable miR-34b/c transfectants significantly showed an increase in the G_0–G_1 fraction ($P < 0.002$) and a decrease in the G_2–M and S fractions ($P < 0.002$), indicating that miR-34b/c induced G_1 cell cycle arrest (Fig. 2D).

MPM stable transfectants and migration, invasion, and motility assay

To estimate the effect of miR-34b/c on migration and invasion potential in MPM, cell migration and invasion was examined using a Boyden chamber. Microscopic images of the Boyden chamber assay are shown in Figure 3A and B. Migration and invasion were significantly suppressed in miR-34b/c stable transfectants, compared with control transfectants. In addition, the effect of miR-34b/c on the motility of MPM cells was estimated using time lapse video microscopy (Fig. 3C). Representative videos are shown in Supplementary Data S1 and S2. The migration velocity was slower in miR-34b/c stable transfectants of H28 and H2052, compared with control transfectants. However, no remarkable difference between miR-34b/c and control transfectants was noted in H290. Although there may be exceptions, on the whole, these results indicated that miR-34b/c was associated with the migration, invasion, and motility of MPM cells.

Adenoviral-mediated p53 and miR-34b/c transfer into cell lines

p53 and p21 were expressed in the 5 MPM cell lines tested (Supplementary Fig. S2). Genotyping data for the *TP53* gene were queried from the database of the Cancer Genome Project, Sanger Institute, Cambridge, UK (www.sanger.ac.uk) to confirm that no *TP53* mutations existed in the all MPM cell lines we used. These data indicate that the wild-type *TP53* gene is present and that p53 is likely functional in MPM cell lines.

To examine the impact of p53 on MPM, we transferred the *TP53* gene using an adenovirus vector (Ad-p53) into MPM (H28, H290, and H2052) and a lung cancer cell line (H125), with mutant *TP53* gene. Western blotting

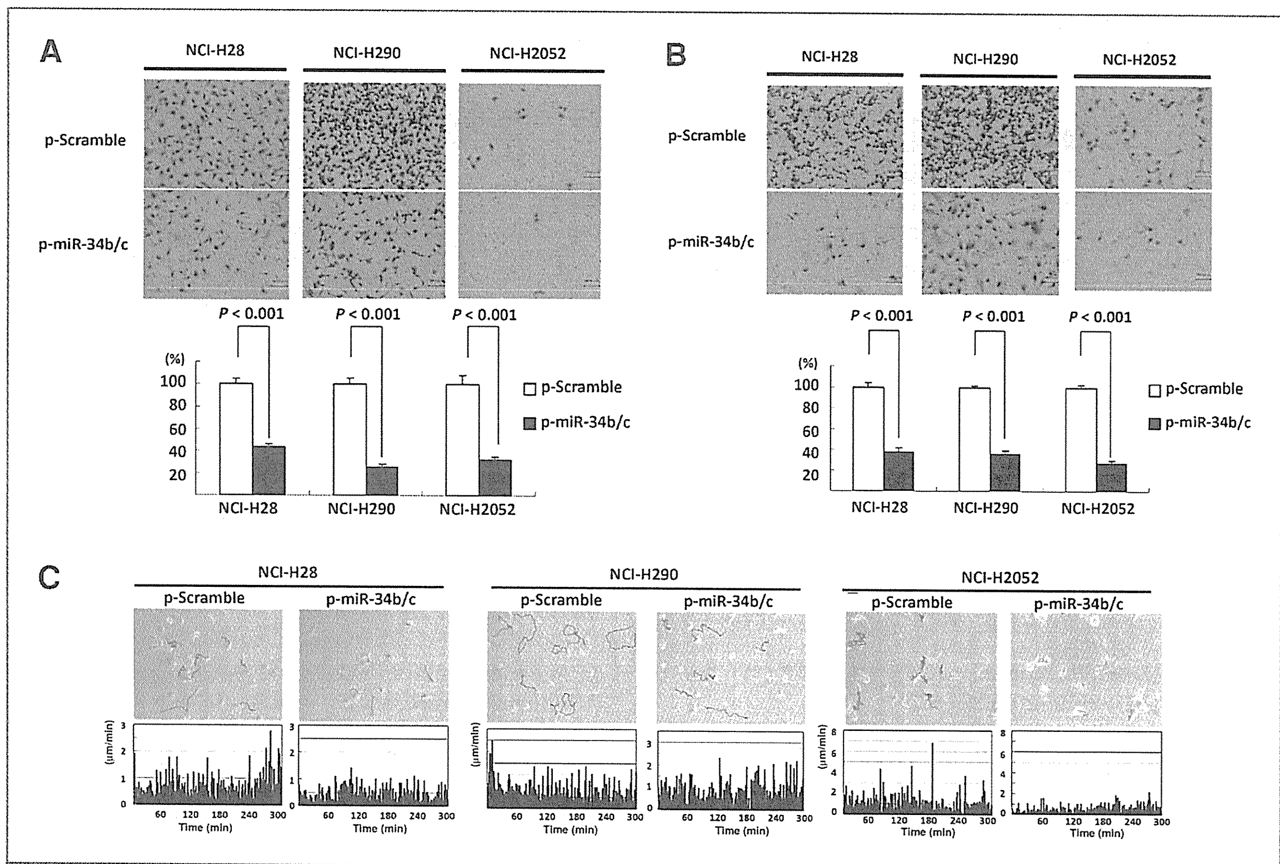

Figure 3. The impact of miR-34b/c on MPM cell migration, invasion, and motility. Representative examples of migration (A) or invasion (B) assay are shown above. The quantitative values expressed as the means ± SD of 5 microscopic fields are representative of 3 experiments (below). C, cell motility was observed under a time-lapse video microscopy. The position of cell nucleus was measured and tracked every minute (0–5 hours) and plotted (red lines; top). The distance that the cell nucleus transversed and velocity for each minute were calculated to determine the speed of the movement in control (p-Scramble) or miR-34b/c–transfected MPM (p-miR-34b/c) cells (bottom).

confirmed that p53 and p21 were upregulated after Ad-p53 transfer (Supplementary Fig. S3: data not shown in H125). Cell viability was examined using an MTS assay. Ad-p53 transfer did not significantly influence the cell viability of the H28, H290, and H2052 cell lines whereas cell viability of H125 was influenced by Ad-p53 (Fig. 4). We also examined the effect of p53 on the expression of miR-34s in MPM and lung cancer cell lines. After Ad-p53 transfer, miR-34b and miR-34c were upregulated in lung cancer cells without miR-34b/c methylation but not in MPM cells with miR-34b/c methylation (Supplementary Table S2).

Next, we transferred Ad-miR-34b/c into cells. Seventy-two hours after Ad-miR-34b/c infection, miR-34b and miR-34c expression were evaluated and the increased expression of both miR-34b and miR-34c was confirmed. The expression values of Ad-miR-34b/c–infected MPMs ranged from 501 to 6,540, as shown in Table 2, part B. These values were much higher than that in nonmalignant mesothelial cells, indicating that adenoviral-mediated miR-34b/c introduction induced miR-34b and miR-34c overexpression. An MTS assay showed that MPM cells infected with Ad-miR-34b/c revealed a significant decrease in cell viability, compared with those infected with Ad-Luc (H28, $P < 0.01$; H290, $P < 0.01$; and H2052, $P < 0.01$; Fig. 4).

Ad-miR-34b/c or Ad-p53 transfer and apoptosis

Western blotting was carried out in MPM cells after Ad-miR-34b/c infection to examine the effect of miR-34b/c overexpression on protein expression. Whereas the results were similar to those in stable transfectants, in which the miR-34b and miR-34c expressions were comparable to physiologic levels, Bcl-2 protein expression was strongly downregulated in Ad-miR-34b/c–infected MPM cell lines (Supplementary Fig. S4). On the basis of these results, cell cycle analysis was conducted to examine whether apoptosis is induced by miR-34b/c using flow cytometry 72 hours after infection. In the H28, H290, and H2052 cell lines, infection with Ad-miR-34b/c caused an increase in the sub-G_0–G_1 DNA content, compared with that in cells infected with Ad-Luc (H28, 5.6%–47.0%; H290; 6.0%–39.9%; H2052, 4.0%–11.5%), indicating the induction of apoptosis (Supplementary Fig. S5). In contrast, Ad-p53 did not induce a drastic change in the

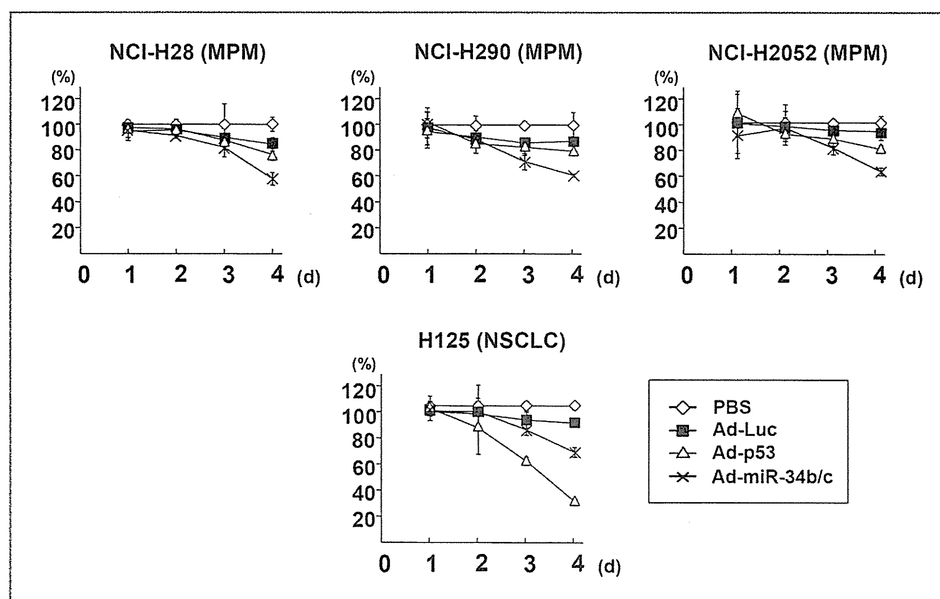

Figure 4. Viability of MPM cells transfected with Ad-Luc (control), Ad-miR-34b/c, or Ad-p53. Cell viability was evaluated by MTS assay. Values are expressed as the means ± SD of 3 experiments.

sub-G_0–G_1 DNA content (H28, 5.6%–7.6%; H290, 6.0%–11.6%; H2052, 4.0%–6.7%).

Discussion

Genetic inactivation of p53 arises in approximately 50% of malignant tumors (28), alteration of *TP53* is rare in MPM (29–31). Indeed, the expression of wild-type p53 and p21, the best-characterized downstream targets of p53, was intact in the MPM cell lines that were used in this study, suggesting that p53 is functional in MPM as previously reported (32, 33). Preclinical experience with mesothelioma cell lines has shown a resistance to *TP53* gene transfer in a number of cell lines (34), indicating that most MPM cells already have functional p53. Also in the present study, *TP53* gene transfer had a minimal effect in MPM cells, whereas miR-34b/c transfer induced apoptosis, producing a significant antitumor effect.

We validated that several genes that have been identified as targets of miR-34b/c, including *c-MET, CDK4, CDK6, CCND1, CCNE2, Bcl-2, c-MYC,* and *E2F3*, were downregulated after the introduction of miR-34b/c. Among the genes that are miR-34b/c targets, *c-MET* was recently reported to be activated in MPM by overexpression or mutation. The suppression of c-MET using MET inhibitors revealed the potent inhibition of proliferation, invasion, and migration in some MPM cell lines (35). Thus, the inhibition of c-MET may contribute to the tumor-suppressive function of miR-34b/c in MPM. Of note, the H2052 cell line, in which c-MET was expressed, was not inhibited by the c-MET inhibitor (35). We confirmed that H2052 was not inhibited by the knockdown of c-MET using siRNA, whereas H28 and H290 were significantly inhibited (Supplementary Fig. S6). However, miR-34b/c introduction inhibited proliferation of H2052. This result suggested that the tumor-suppressive effect of miR-34b/c on MPM resulted from the downregulation of multiple oncogenic genes that are directly or indirectly regulated by miR-34b/c, which implies that miRNA such as miR-34b/c may be much more efficient and effective for a therapeutic target rather than an individual gene such as *c-MET*.

Our results also showed that cell cycle arrest and induction of apoptosis were caused by miR-34b/c. A subset of genes known as cell cycle and transcriptional regulators were also downregulated with miR-34b/c introduction (9, 12). *CDK4, CDK6, CCND1,* and *CCNE2* are regulators of cell cycle and are required for the transition from G_1–S-phase (36). Among them, *CDK4* is negatively regulated by $p16^{INK4A}$, which is deleted in the majority of MPMs (29). Frizelle and colleagues showed that the reexpression of $p16^{INK4A}$ induced G_1 cell cycle arrest and apoptosis in MPM (37). Thus, the inhibition of CDK4 along with other cell cycle regulators is considered to lead to the induction of cell cycle arrest and the subsequent inhibition of proliferation in MPM.

The antiapoptotic potential of MPM makes it highly resistant to chemotherapeutic agents and radiation (2). Wild-type p53 causes G_1 cell cycle arrest, allowing damage to be repaired before replication or triggering apoptosis if the damage cannot be repaired (38). In MPM, which has wild-type *TP53* gene, resistance to apoptosis has been considered to arise downstream of p53. Bcl-2 is an antiapoptotic protein located downstream of p53. Overexpression of Bcl-2 in MPM tumor has been reported from 8% to 40% (39, 40) and 4 of 6 MPM cell lines seem to exhibit Bcl-2 overexpression in our study (Supplementary Fig. S2). In miR-34b/c stable transfectants, Bcl-2 did not seem to be downregulated, compared with control transfectants. Because stable transfectants are derived from selected clones that survive after miR-34b/c transfection, stable transfectants are not appropriate for examining the effect of miR-34b/c on apoptosis. Thus, whereas Ad-miR-34b/c

transfer led to overexpression of miR-34b and miR-34c and induced apoptosis with the downregulation of Bcl-2, whether physiologic levels of miR-34b/c expression are capable of downregulating Bcl-2 in MPM remains unknown.

In this study, we used stable transfectants and adenoviral-infected cells. Our stable transfectants with physiologic expression values of miR-34b and miR-34c would be appropriate models for investigating the pathogenic role of miR-34b/c in MPM. Using this system, the restoration of the miR-34b and miR-34c suppressed oncologic features of MPM, including cell proliferation and invasiveness, strongly suggests that the silencing of miR-34b/c by methylation is a key alteration in MPM. On the other hand, the adenoviral system induced elevated miR-34b and miR-34c expression possibly induced apoptosis, suggesting the therapeutic possibility of miR-34b/c transfer for MPM.

Many functionally validated miRNAs target oncogenes and tumor suppressors. Moreover, gain or loss of function of individual miRNA has been reported to affect tumor cell proliferation, apoptosis, and invasion (41, 42). Therefore, it is thought that normalization of miRNA expression could be a potential method of therapeutic intervention. As miR-34b/c acts as a tumor suppressor, its expression should be restored in targeted tumor cells by the delivery. Delivery systems for miRNA to access tumor cells are available, including viral or liposomal delivery (43, 44).

Because MPM is one of the most difficult malignancies to treat, it is significant that the current study suggests a potential utility of miR-34b/c as a therapeutic option. Combination of miR-34b/c delivery and existing conventional therapies could be synergistic. Because miR-34b/c recovers several crucial functions in p53 pathway, miR-34b/c may increase the sensitivity of tumor cells for conventional antitumor agents or radiation. Further investigations are warranted for applying the miR-34b/c to novel therapeutic strategies.

In conclusion, our results show that miR-34b/c is frequently downregulated by aberrant methylation in MPM, resulting in the loss of tumor-suppressive p53 function and the acquisition of a malignant phenotype. miR-34b/c plays an important role in the pathogenesis of MPM, and the epigenetic silencing of miR-34b/c might explain why p53 functions are impaired in MPM despite the presence of intact p53 in the majority of MPM. Our study provides new insights into the molecular pathogenesis of MPM and suggests that miR-34b/c can be a potential therapeutic target for MPM.

Disclosure of Potential Conflict of Interest

No potential conflicts of interest were disclosed.

Acknowledgments

The authors thank Dr. Adi F. Gazdar, Hamon Center for Therapeutic Oncology Research and Department of Pathology, University of Texas Southwestern Medical Center at Dallas, for providing the cell lines that were used in this study.

Grant Support

This study was supported by Grant-in-Aids for Scientific Research from the Ministry of Education, Culture, Sports, Science and Technology of Japan 22591566 (S. Toyooka) and for the 13 fields of occupational injuries and illnesses of the Japan Labor Health and Welfare Organization (T. Kishimoto).

The costs of publication of this article were defrayed in part by the payment of page charges. This article must therefore be hereby marked *advertisement* in accordance with 18 U.S.C. Section 1734 solely to indicate this fact

Received November 14, 2010; revised May 23, 2011; accepted June 4, 2011; published OnlineFirst June 14, 2011.

References

1. Spirtas R, Heineman EF, Bernstein L, Beebe GW, Keehn RJ, Stark A, et al. Malignant mesothelioma: attributable risk of asbestos exposure. Occup Environ Med 1994;51:804–11.
2. Robinson BW, Musk AW, Lake RA. Malignant mesothelioma. Lancet 2005;366:397–408.
3. Cote RJ, Jhanwar SC, Novick S, Pellicer A. Genetic alterations of the p53 gene are a feature of malignant mesotheliomas. Cancer Res 1991;51:5410–6.
4. Metcalf RA, Welsh JA, Bennett WP, Seddon MB, Lehman TA, Pelin K, et al. p53 and Kirsten-ras mutations in human mesothelioma cell lines. Cancer Res 1992;52:2610–5.
5. Shimamura A, Fisher DE. p53 in life and death. Clin Cancer Res 1996;2:435–40.
6. Bartel DP. MicroRNAs: genomics, biogenesis, mechanism, and function. Cell 2004;116:281–97.
7. Lu J, Getz G, Miska EA, Alvarez-Saavedra E, Lamb J, Peck D, et al. MicroRNA expression profiles classify human cancers. Nature 2005;435:834–8.
8. Garzon R, Calin GA, Croce CM. MicroRNAs in cancer. Annu Rev Med 2009;60:167–79.
9. He L, He X, Lim LP, de Stanchina E, Xuan Z, Liang Y, et al. A microRNA component of the p53 tumour suppressor network. Nature 2007;447:1130–4.
10. Bommer GT, Gerin I, Feng Y, Kaczorowski AJ, Kuick R, Love RE, et al. p53-mediated activation of miRNA34 candidate tumor-suppressor genes. Curr Biol 2007;17:1298–307.
11. Corney DC, Flesken-Nikitin A, Godwin AK, Wang W, Nikitin AY. MicroRNA-34b and MicroRNA-34c are targets of p53 and cooperate in control of cell proliferation and adhesion-independent growth. Cancer Res 2007;67:8433–8.
12. Hermeking H. p53 enters the microRNA world. Cancer Cell 2007;12:414–8.
13. Murthy SS, Shen T, De Rienzo A, Lee WC, Ferriola PC, Jhanwar SC, et al. Expression of GPC3, an X-linked recessive overgrowth gene, is silenced in malignant mesothelioma. Oncogene 2000;19:410–6.
14. Merlo A, Herman JG, Mao L, Lee DJ, Gabrielson E, Burger PC, et al. 5′ CpG island methylation is associated with transcriptional silencing of the tumour suppressor p16/CDKN2/MTS1 in human cancers. Nat Med 1995;1:686–92.
15. Saito Y, Liang G, Egger G, Friedman JM, Chuang JC, Coetzee GA, et al. Specific activation of microRNA-127 with downregulation of the proto-oncogene BCL6 by chromatin-modifying drugs in human cancer cells. Cancer Cell 2006;9:435–43.
16. Lujambio A, Ropero S, Ballestar E, Fraga MF, Cerrato C, Setién F, et al. Genetic unmasking of an epigenetically silenced microRNA in human cancer cells. Cancer Res 2007;67:1424–9.

17. Toyota M, Suzuki H, Sasaki Y, Maruyama R, Imai K, Shinomura Y, et al. Epigenetic silencing of microRNA-34b/c and B-cell translocation gene 4 is associated with CpG island methylation in colorectal cancer. Cancer Res 2008;68:4123–32.
18. Lodygin D, Tarasov V, Epanchintsev A, Berking C, Knyazeva T, Körner H, et al. Inactivation of miR-34a by aberrant CpG methylation in multiple types of cancer. Cell Cycle 2008;7:2591–600.
19. Busacca S, Germano S, De Cecco L, Rinaldi M, Comoglio F, Favero F, et al. MicroRNA signature of malignant mesothelioma with potential diagnostic and prognostic implications. Am J Respir Cell Mol Biol 2010;42:312–9.
20. Guled M, Lahti L, Lindholm PM, Salmenkivi K, Bagwan I, Nicholson AG, et al. CDKN2A, NF2, and JUN are dysregulated among other genes by miRNAs in malignant mesothelioma -A miRNA microarray analysis. Genes Chromosomes Cancer 2009;48:615–23.
21. Pass HI, Goparaju C, Ivanov S, Donington J, Carbone M, Hoshen M, et al. hsa-miR-29c* is linked to the prognosis of malignant pleural mesothelioma. Cancer Res 2010;70:1916–24.
22. Toyooka S, Pass HI, Shivapurkar N, Fukuyama Y, Maruyama R, Toyooka KO, et al. Aberrant methylation and simian virus 40 tag sequences in malignant mesothelioma. Cancer Res 2001;61: 5727–30.
23. Gandhi J, Zhang J, Xie Y, Soh J, Shigematsu H, Zhang W, et al. Alterations in genes of the EGFR signaling pathway and their relationship to EGFR tyrosine kinase inhibitor sensitivity in lung cancer cell lines. PLoS One 2009;4:e4576.
24. Ramirez RD, Sheridan S, Girard L, Sato M, Kim Y, Pollack J, et al. Immortalization of human bronchial epithelial cells in the absence of viral oncoproteins. Cancer Res 2004;64:9027–34.
25. Herman JG, Graff JR, Myohanen S, Nelkin BD, Baylin SB. Methylation-specific PCR: a novel PCR assay for methylation status of CpG islands. Proc Natl Acad Sci U S A 1996;93:9821–6.
26. Ji Q, Hao X, Zhang M, Tang W, Yang M, Li L, et al. MicroRNA miR-34 inhibits human pancreatic cancer tumor-initiating cells. PLoS One 2009;4:e6816.
27. He TC, Zhou S, da Costa LT, Yu J, Kinzler KW, Vogelstein B. A simplified system for generating recombinant adenoviruses. Proc Natl Acad Sci U S A 1998;95:2509–14.
28. Hollstein M, Sidransky D, Vogelstein B, Harris CC. p53 mutations in human cancers. Science 1991;253:49–53.
29. Prins JB, Williamson KA, Kamp MM, Van Hezik EJ, Van der Kwast TH, Hagemeijer A, et al. The gene for the cyclin-dependent-kinase-4 inhibitor, CDKN2A, is preferentially deleted in malignant mesothelioma. Int J Cancer 1998;75:649–53.
30. Sekido Y. Molecular biology of malignant mesothelioma. Environ Health Prev Med 2008;13:65–70.
31. Toyooka S, Kishimoto T, Date H. Advances in the molecular biology of malignant mesothelioma. Acta Med Okayama 2008;62:1–7.
32. Hopkins-Donaldson S, Belyanskaya LL, Simões-Wüst AP, Sigrist B, Kurtz S, Zangemeister-Wittke U, et al. p53-induced apoptosis occurs in the absence of p14(ARF) in malignant pleural mesothelioma. Neoplasia 2006;8:551–9.
33. Gordon GJ, Rockwell GN, Jensen RV, Rheinwald JG, Glickman JN, Aronson JP, et al. Identification of novel candidate oncogenes and tumor suppressors in malignant pleural mesothelioma using large-scale transcriptional profiling. Am J Pathol 2005;166: 1827–40.
34. Pataer A, Smythe WR, Yu R, Fang B, McDonnell T, Roth JA, et al. Adenovirus-mediated Bak gene transfer induces apoptosis in mesothelioma cell lines. J Thorac Cardiovasc Surg 2001;121: 61–7.
35. Jagadeeswaran R, Ma PC, Seiwert TY, Jagadeeswaran S, Zumba O, Nallasura V, et al. Functional analysis of c-Met/hepatocyte growth factor pathway in malignant pleural mesothelioma. Cancer Res 2006;66:352–61.
36. Aggarwal BB, Ichikawa H. Molecular targets and anticancer potential of indole-3-carbinol and its derivatives. Cell Cycle 2005;4: 1201–15.
37. Frizelle SP, Kratzke MG, Carreon RR, Engel SC, Youngquist L, Klein MA, et al. Inhibition of both mesothelioma cell growth and Cdk4 activity following treatment with a TATp16INK4a peptide. Anticancer Res 2008;28:1–7.
38. Oren M. Decision making by p53: life, death and cancer. Cell Death Differ 2003;10:431–42.
39. Soini Y, Kinnula V, Kaarteenaho-Wiik R, Kurttila E, Linnainmaa K, Paakko P. Apoptosis and expression of apoptosis regulating proteins bcl-2, mcl-1, bcl-X, and bax in malignant mesothelioma. Clin Cancer Res 1999;5:3508–15.
40. O'Kane SL, Pound RJ, Campbell A, Chaudhuri N, Lind MJ, Cawkwell L. Expression of bcl-2 family members in malignant pleural mesothelioma. Acta Oncol 2006;45:449–53.
41. Calin GA, Croce CM. MicroRNA signatures in human cancers. Nat Rev Cancer 2006;6:857–66.
42. Spizzo R, Nicoloso MS, Croce CM, Calin GA. SnapShot: microRNAs in cancer. Cell 2009;137:586–e1.
43. Chung KH, Hart CC, Al-Bassam S, Avery A, Taylor J, Patel PD, et al. Polycistronic RNA polymerase II expression vectors for RNA interference based on BIC/miR-155. Nucleic Acids Res 2006;34:e53.
44. Stegmeier F, Hu G, Rickles RJ, Hannon GJ, Elledge SJ. A lentiviral microRNA-based system for single-copy polymerase II-regulated RNA interference in mammalian cells. Proc Natl Acad Sci U S A 2005;102:13212–7.

Clinical study of asbestos-related lung cancer in Japan with special reference to occupational history

Takumi Kishimoto,[1,6] Kenichi Gemba,[1] Nobukazu Fujimoto,[1] Kazuo Onishi,[2] Ikuji Usami,[3] Keiichi Mizuhashi[4] and Kiyonobu Kimura[5]

[1]Okayama Rosai Hospital, Okayama; [2]Kobe Rosai Hospital, Kobe; [3]Asahi Rosai Hospital, Owariasahi; [4]Toyama Rosai Hospital, Uozu; [5]Hokkaido Central Rosai Hospital, Iwamizawa, Japan

(Received November 29, 2009/Revised January 11, 2010/Accepted January 18, 2010/Online publication March 10, 2010)

A total of 152 patients with asbestos-related lung cancer recognized by the criteria of Japanese compensation law for asbestos-related diseases were examined and compared with 431 patients with non-asbestos-related lung cancer. Male comprised 96% of patients. Ages ranged from 50 to 91 years with a median of 72 years. Eighty-nine percent were smokers or ex-smokers. Almost all patients had occupational histories of asbestos exposure. The median duration of asbestos exposure was 31 years and the median latency period was 47 years. Thirty-four percent of patients exhibited asbestosis and 81% exhibited pleural plaques by radiography. Regarding asbestos particles in the lung for 73 operated or autopsied patients, 62% had more than 5,000 particles per gram. On the other hand, 100% of non-asbestos-related lung cancer patients had <5000 particles per gram with a median of 554 particles. The number of asbestos bodies in the lung, male gender, absence of symptoms, smoking index, and early stage of cancer were significantly much more than those of non-asbestos-related lung cancer. In this study, a diagnosis of asbestos-related lung cancer was made in 34% of patients by asbestosis, in 62% by presence of both pleural plaques and more than 10 years' occupational asbestos exposure, and in 4% by more than 5000 asbestos particles per gram of lung tissue. Occupational histories, duration of asbestos exposure, and pleural plaques are common categories for the recognition of asbestos-related lung cancer in Japan. (*Cancer Sci* 2010; 101: 1194–1198)

The disaster of asbestos exposure has been a serious social problem in Japan since 2005,[1] with neighborhood exposure to asbestos inducing mesothelioma in more than 100 patients in the Amagasaki area. Furthermore, the number of patients with mesothelioma and asbestos-related lung cancer (Fig. 1) has recently increased. In this study, clinical features and occupational histories for asbestos-related lung cancer patients in Japan were investigated and compared with those of non-asbestos-related lung cancer patients.

Materials and Methods

In this study, the definition of asbestos-related lung cancer was primary lung cancer with the following: (i) asbestosis on chest radiography; (ii) pleural plaques with more than 10 years' occupational asbestos exposure; (iii) asbestos particles or fibers on the lung tissues with more than 10 years' occupational asbestos exposure; and (iv) more than 5000 asbestos particles per gram of dry lung tissue with occupational asbestos exposure. These criteria fulfill the Japanese compensation law of asbestos-related lung cancer.

Retrospective study of asbestos-related lung cancer patients from 2000 to 2008 treated in 18 Rosai hospitals throughout Japan was performed. Gender, age, diagnostic motive, smoking history, histological type of lung cancer, clinical stage, therapeutic procedures and prognosis, occupational history, and radiological findings of asbestos-related changes were examined.

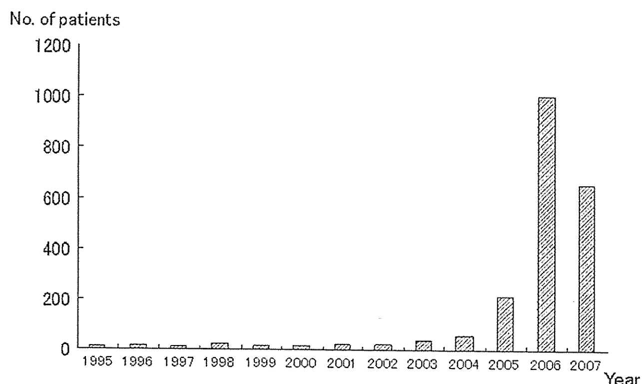

Fig. 1. Number of asbestos-related lung cancer in Japan from 1995 to 2007 was shown in this figure. The number of patients with asbestos-related lung cancer has drastically increased after the 2005 Kubota Shock. (Data from statistics published by the Ministry of Health, Labor, and Welfare of Japan.)

Non-asbestos-related lung cancer patients treated in Okayama Rosai hospital from 1997 to 2007[2] were also examined for gender, age, smoking history, histological type of lung cancer, clinical stage, and therapeutic procedures and prognosis. Non-asbestos-related lung cancer does not fulfill the criteria for the Japanese compensation law of asbestos-related lung cancer. The findings of asbestos-related changes such as pleural plaques were examined by chest X-ray and chest computed tomography (CT) (including high resolution computed tomography (HRCT)) for all patients with asbestos-related lung cancer and non-asbestos-related lung cancer. Prognosis of asbestos-related lung cancer was calculated by the complication of asbestosis. Prognostic factors in both asbestos-related and non-asbestos-related lung cancers were calculated by multivariate analysis.

The number of asbestos particles was counted for the operated or autopsied patients (73 patients with asbestos-related and 23 with non-asbestos-related lung cancers). The number of asbestos particles in the lung was counted by the method of Kohyama.[3] One to 2 *g* of lung tissue without cancer invasion was dissolved in sodium hypochlolite and 5% potassium hydroxide (KOH) for 12 h, and complete dissolution of the lung tissue was confirmed. The supernatant was discarded, the sediment was dissolved with 10 mL of chloroform and 50% ethanol, and the solution was centrifuged at 18G for 5 min. The supernatant was discarded, the sediment was dissolved with 95% ethanol, the solution was passed through a Millipore filter, and the asbestos particles on the filter were counted under phase-contrasted microscope at

[6]To whom correspondence should be addressed.
E-mail: nakisimt@okayamaH.rofuku.go.jp

doi: 10.1111/j.1349-7006.2010.01509.x
© 2010 Japanese Cancer Association

×200 magnification. The number of asbestos particles per gram of dry lung tissue was then calculated. The data were statistically analyzed, using Student's t-test and $P < 0.05$ was regarded as statistically significant.

Results

A total of 152 patients with asbestos-related lung cancer were examined in this study. Regarding gender, 146 were male and six were female. Ages ranged from 50 to 91 years with a median of 72 years. Sixty-four patients were diagnosed by the chief complaints of dyspnea, cough, etc. Fifty-nine patients were diagnosed by regular health check-up and another 20 patients were accidentally diagnosed during the following of other diseases. For nine patients there was no information. Only 15 patients (10%) were non-smokers and another 134 were smokers or ex-smokers. The smoking index for 149 patients ranged from 0 to 2550 with a median of 900. The smoking index for 71 patients exceeded 1000. The smoking history of three patients was unknown (Table 1).

Table 1. Characteristics of asbestos-related and non-asbestos-related lung cancers

	Asbestos-related lung cancers (n = 152)	Non-asbestos-related lung cancers (n = 431)	P-values
Gender	(%)	(%)	<0.01
Male	146 (96.1)	311 (72.2)	
Female	6 (3.9)	120 (27.8)	
Age (years)			
<50	0	25 (5.8)	0.09
50–59	16 (10.5)	70 (16.2)	
60–69	41 (27.0)	110 (25.5)	
70–79	62 (40.8)	153 (35.5)	
≥80	33 (21.7)	73 (16.9)	
Symptom			
Absent	79 (55.2)	172 (39.9)	<0.01
Present	64 (44.8)	259 (60.1)	
Smoking habit			
Never smoker	15 (9.9)	88 (20.4)	<0.01
Smoker	134 (90.1)	343 (79.6)	
BI ≥ 1000	71 (47.0)	133 (30.9)	
Pathology			
Adenocarcinoma	85 (55.9)	238 (55.2)	
Squamous cell carcinoma	39 (25.7)	86 (20.0)	
Small cell carcinoma	18 (11.8)	72 (16.7)	0.07
Others	10 (6.6)	35 (8.1)	
Stage			
IA	33 (22.4)	68 (15.8)	<0.01
IB	17 (11.6)	30 (7.0)	
IIA	3 (2.0)	3 (0.7)	
IIB	5 (3.4)	20 (4.6)	
IIIA	9 (6.1)	33 (7.7)	
IIIB	35 (23.8)	123 (28.5)	
IV	45 (30.6)	154 (35.7)	
Therapeutic procedure			
Operation	53 (34.9)	100 (23.2)	0.06
Chemotherapy	56 (36.8)	187 (43.4)	
Chemo. + radiotherapy	12 (7.9)	67 (15.5)	
Others	8 (5.3)	25 (5.8)	
Best supportive care	23 (15.1)	52 (12.1)	

BI, Brinkmann index.

Regarding the histology of 143 patients with asbestos-related lung cancer, 85 exhibited adenocarcinoma, 39 had squamous-cell type, 18 had small-cell type, and one had large-cell type. The histological types of nine patients were not determined. The features of non-asbestos-related lung cancer are described in Table 1. Rates of male gender, being symptom free, smoking, and early stage disease for asbestos-related lung cancer are significantly ($P > 0.01$) higher than those of non-asbestos-related lung cancer.

The survival term was overall 17.4 months with 57.0% having 1 year-survival and 25% having 5 year-survival. On the other hand, the survival term for 431 patients with non-asbestos-related lung cancer was 19.2 months with 70.1% having 1 year-survival and 24.5% of having year-survival. The difference in survival term between the two groups was not statistically significant (Fig. 2). Three patients with asbestos-related lung cancer died within 3 months of surgery and another four patients died from respiratory failure due to advanced asbestosis. Two of three patients with asbestosis were did not have good survival after surgery because of acute exacerbation of asbestosis. However, the survival of 51 patients with asbestosis was 17.2 months and that of 101 patients without asbestosis was 18.1 months; there was no statistical significance in either group. Prognostic factors calculated by multivariate analysis in both groups, included age, gender, and stages, but not asbestos exposure or pathology (Table 2).

Regarding therapy, 53 patients underwent surgery; 56 received chemotherapy, with nine receiving a combination of surgery and chemotherapy; 16 received radiation, with 12 receiving a combination of chemotherapy and radiation; and 23 received the best available supportive care. These numbers resemble those for non-asbestos-related lung cancer. Survival for patients who received surgery was 55.1 months with 45% having 5-year survival; and for radiation, chemotherapy, and best supportive care, survival was 9.3 months, 10.3 months, and 7.0 months, respectively.

One hundred and fifty (98%) of 152 patients whose occupational histories were ascertained had occupational exposure to asbestos. For another two patients with more than 5000 asbestos particles in the lung, occupational histories were not confirmed. Thirty-four patients had occupational histories of shipyard work, 29 had construction work, 15 had exposure due to making asbestos products, 15 had piping works, and 14 had insulation work, with the remainder also having been employed in asbestos-related work (Table 3).

Age at exposure to asbestos for the first time ranged from 14 to 50 years with a median of 21 years. The duration of asbestos exposure for 146 patients ranged from 1 to 60 years with a median of 31 years, and the latency period from first exposure to the appearance of lung cancer ranged from 5 to 71 years with a median of 47 years.

Regarding the radiographical findings of asbestos-related changes, only 51 patients (34%) exhibited asbestosis; 122 (81%) exhibited pleural plaques and 100 (66%) showed calcified plaques. Seven patients exhibited rounded atelectasis and four diffuse pleural thickening. Only 33 patients (22%) had complicated pleural effusion (Table 4). Thirty-two patients with asbestosis were exposed to asbestos due to work in asbestos product making, insulation, and asbestos spraying. And other 19 patients were exposed to asbestos due to work in shipyards and construction work and work with piping. Ninety-four patients (62%) with asbestos-related lung cancer were diagnosed by the presence of pleural plaques and had more than 10 years' occupational asbestos exposure (Fig 4). On the other hand, 10 patients with non-asbestos-related lung cancer showed pleural plaques, but no other findings such as asbestosis or diffuse pleural thickening.

As for the number of asbestos particles in the lung in 73 patients, 45 (62%) had more than 5000 asbestos bodies per gram

© 2010 Japanese Cancer Association

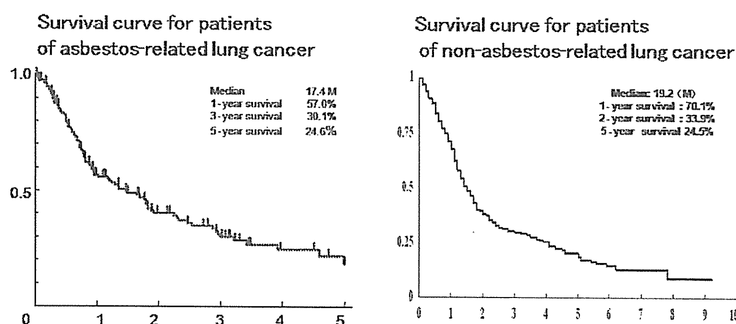

Fig. 2. Survival curves for asbestos-related lung cancer and non-asbestos-related lung cancer show almost the same pattern which indicates almost the same rates of survival between these two types of lung cancer.

of dry lung tissue which meant they had an occupational history of asbestos exposure. Furthermore, 21 (29%) exceeded 50 000 particles which meant heavy exposure. Seven (4%) were diagnosed with more than 5000 asbestos particles per gram of lung tissue (Fig. 4). However, 14 (19%) had <1000 asbestos particles which indicated the non-exposed citizen level. These 14 patients had pleural plaques with more than 10 years' occupational asbestos exposure and were diagnosed with asbestos-related lung cancer.

Among 18 asbestosis patients, 10 (56%) exceeded 50 000 particles, but two patients had <5000 particles. On the other hand, for 55 patients without asbestosis, 14 had <1000 particles and 11 (20%) exceeded 50 000 particles (Fig. 3). Twenty-three patients with non-asbestos-related lung cancer had 0 to 3751 asbestos particles per gram of lung tissue with a median of 554 particles.

Discussion

Asbestos is known to be carcinogenic for malignant mesothelioma and lung cancer. It has been established that exposure to asbestos can induce malignant mesothelioma. Regarding the onset of primary lung cancer, the involvement of smoking has been emphasized.[4] Asbestos enhances the mutagenicity of tobacco carcinogen and it acts independently to tissue damage responsible for fibrosis, that is asbestosis.[5] High incidences of lung cancer among individuals exposed to asbestos have been demonstrated by various cohort studies.[3] The present study was undertaken to characterize primary lung cancer observed in asbestos-exposed individuals in Japan and to examine these patients for the presence or absence of concomitant lung lesions such as asbestosis and pleural plaques. While no definition of asbestos-related lung cancer has been established, Helsinki criteria[6] indicates that having 25 asbestos fiber-years doubles the risk of lung cancer.

The present study adopted the criteria of asbestos-related lung cancer defined by the Japanese compensation law of asbestos-related diseases in 2006. A total of 152 patients with asbestos-related lung cancer were examined and the median age was 72 years which was 7 years older than that of a group with Japanese malignant pleural mesothelioma described in 2004.[7] Ninety-six percent of them were males who had occupational histories of asbestos exposure, and the median duration of asbestos exposure was 31 years. Forty-two percent were diagnosed by subjective complaints, but another 68% were diagnosed during regular check-ups or accidentally diagnosed due to abnormal chest shadows without subjective complaints. This data seems to be due to the Japanese system of having regular check-ups for lung cancer, because 60% of patients with non-asbestos-related lung cancer were diagnosed by subjective complaints.

Regarding smoking, only 15 patients (10%) were non-smokers and 134 were smokers or ex-smokers. Seventy-one patients (47%) exceeded the smoking index of 1000 which meant they

Table 2. Univariate and multivariate analysis for the prognosis of asbestos and non-asbestos-related lung cancer

Univariate analysis				
Factors		*n*	MST (95% CI)	Log-rank test
Asbestos	Related	152	16.2 months (8.3–24.1)	*P* = 0.673
	Non-related	431	17.2 months (15.1–19.3)	
Age	≤70	278	20.8 months (15.9–25.7)	*P* < 0.001
(years)	71+	305	14.1 months (11.7–16.5)	
Gender	Male	457	15.4 months (13.7–17.1)	*P* < 0.001
	Female	126	24.5 months (17.8–31.2)	
Pathology	NSCLC	493	18.1 months (15.4–20.8)	*P* = 0.001
	SCLC	90	13.4 months (11.1–15.7)	
Stage	I–II	179	21.5 months (17.7–25.3)	*P* < 0.001
	III–IV	399	13.4 months (11.1–15.7)	

Multivariate analysis			
Factors	Exp (β)	95% CI	*P*-values
Asbestos	1.051	0.816–1.353	0.699
Age	1.625	1.312–2.013	<0.001
Gender	1.686	1.255–2.273	0.001
Pathology	1.290	0.973–1.710	0.077
Stage	1.945	1.548–2.443	<0.001

CI, confidence interval; MST, median survival term; NSCLC, non-small-cell lung cancer; SCLC, small-cell lung cancer.

Table 3. Occupational histories of asbestos-related lung cancer patients

Area of occupation	*n*
Shipbuilding	34
Construction	29
Asbestos product making	15
Piping	15
Insulation	14
Electrician	8
Chemicals	6
Arc welding	5
Transportation	4
Steel company	4
Asbestos spraying	3
Fire bricklaying	3
Automobile making	3
Metal making	2
Furnace making	2
Warehousing	1
Casting	1
Other	1

doi: 10.1111/j.1349-7006.2010.01509.x
© 2010 Japanese Cancer Association

Table 4. **Radiological findings in asbestos-related diseases**

Findings	n (%)
Asbestosis	51 (34.0)
Pleural plaques	122 (81.3)
Calcified PQ	81 (73.6)
Rounded atelectasis	7 (4.7)
Diffuse pleural thickening	4 (2.7)
Pleural effusion	33 (22.3)

PQ, pleural plaque.

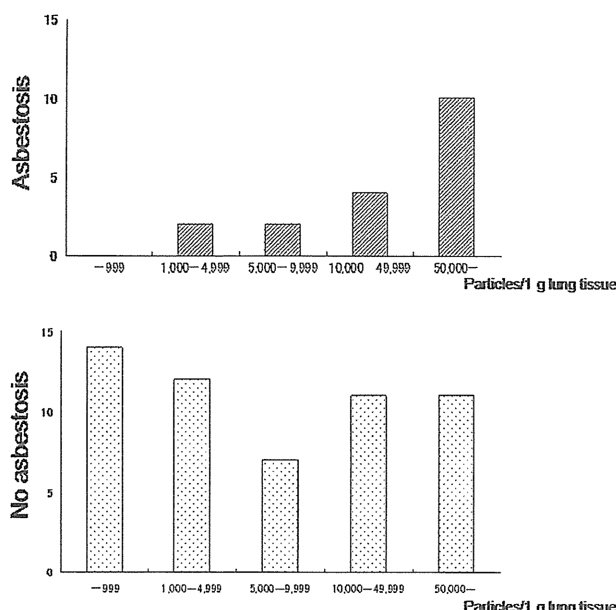

Fig. 3. Number of asbestos particles per gram of lung tissue for asbestosis and non-asbestosis by chest X-ray. For asbestosis, two patients (11.1%) had <5000 asbestos particles; 14 (77.8%) had more than 10 000 particles; while 10 had more than 50 000 particles (55.6%) which means heavy asbestos exposure. On the other hand, for non-asbestosis, 31 patients had more than 5000 particles and 14 had <1000 particles. For the patients with non-asbestosis, no particular pattern in number of asbestos particles could be observed.

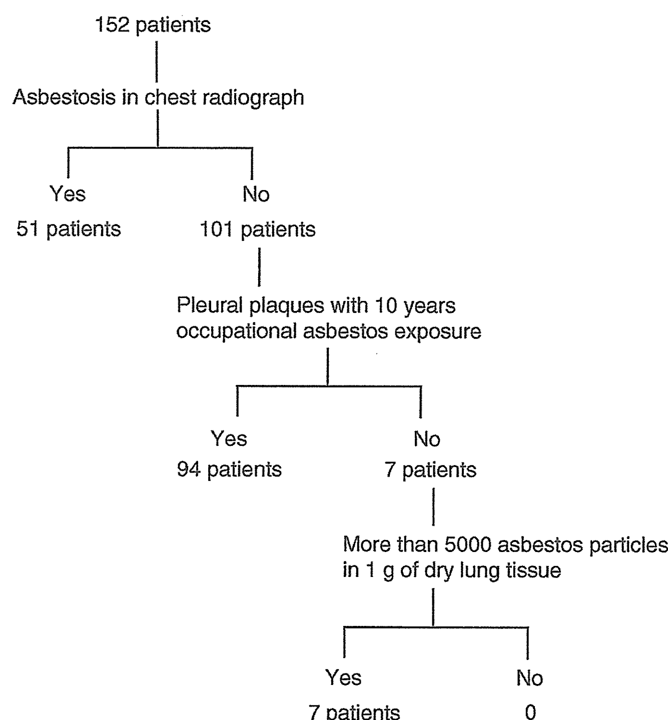

Fig. 4. Flow chart of asbestos-related lung cancer diagnoses.

were heavy smokers. Lung cancer can occur in nonsmokers exposed to asbestos; however, the risk is magnified several-fold by smoking,[8] and increased risk for lung cancer remains up to 20 years after cessation of smoking.[9] Forty-seven percent of our patients were heavy smokers whose lung cancer was suggested to be related not only to asbestos exposure but also to smoking. Ex-smokers stopped smoking within 20 years of the appearance of lung cancer.

Histological classification of asbestos-related lung cancer indicated that 59% had adenocarcinoma and 27% had squamous cell type, which is a similar pattern to that of non-asbestos-related lung cancer (control group) in Japan.

Overall survival of 152 patients with asbestos-related lung cancer was 17.4 months with 25% having 5 year-survival. This data is similar that of the control group which had an overall survival of 19.2 months with 25% having 5-year survival. As for therapeutic procedures, the survival for patients who underwent surgery was 55.1 months with a 5-year survival rate of 45% and that of chemotherapy was 10.3 months. Lung cancer which shows limited small areas of ground glass opacity by CT scanning is typically early stage; therefore, the survival of this type is better after surgery. These data showed that therapeutic procedures for asbestos-related lung cancer and survival were also similar to controls. Some patients with early stage experienced the exacerbation of asbestosis after surgery. But the presence of asbestosis did not affect the survival of those with asbestos-related lung cancer. Prognostic factors of survival for asbestos-related and non-asbestos-related lung cancers by multivariate analysis proved not to be asbestos exposure or pathology, but rather age, gender, and stage.

As for occupational history, shipyard workers, asbestos product makers, piping workers, and insulation workers mainly comprised asbestos-related lung cancer patients, which was similar to that for malignant mesothelioma as described previously). Thirty-four patients who were shipyard workers with more than 10-year occupational histories were considered as proof of moderate density of exposure to asbestos. Insulation workers, asbestos product makers, and piping workers were considered to have had heavy exposure to asbestos. The term of exposure to asbestos ranged from 1 to 60 years with a median of 31 years. Workers who were suggested to have had heavy exposure to asbestos through insulation or asbestos spraying tended to have had short-term exposure, and construction workers thought to have had lower levels of exposure tended to have had longer histories of asbestos exposure. The latency period had a median of 47 years which is longer than that of malignant mesothelioma (37 years)[6] and that of asbestos-related-lung cancer patients (43 years) who were treated in several Rosai Hospitals from 1995 to 2000.[10]

Regarding the radiological findings for asbestos-related changes, 34% of patients had complicated asbestosis, but 81% had pleural plaques which occurred even due to low density of asbestos exposure, which was about same percent as Bianchi's data.[11] Sixty-two percent of patients were diagnosed as having asbestos-related lung cancer on the evidence of both pleural plaques and 10 years' occupational asbestos exposure. Ten patients with non-asbestos-related lung cancer also exhibited pleural plaques, but no evidence of enough asbestos particles or

© 2010 Japanese Cancer Association